

Saddle point preconditioners for weak-constraint 4D-Var

Jemima M. Tabcart and John W. Pearson

May 17, 2021

Abstract

Data assimilation algorithms combine information from observations and prior model information to obtain the most likely state of a dynamical system. The linearised weak-constraint four-dimensional variational assimilation problem can be reformulated as a saddle point problem, in order to exploit highly-parallel modern computer architectures. In this setting, the choice of preconditioner is crucial to ensure fast convergence and retain the inherent parallelism of the saddle point formulation. We propose new preconditioning approaches for the model term and observation error covariance term which lead to fast convergence of preconditioned Krylov subspace methods, and many of these suggested approximations are highly parallelisable. In particular our novel approach includes model information in the model term within the preconditioner, which to our knowledge has not previously been considered for data assimilation problems. We develop new theory demonstrating the effectiveness of the new preconditioners for a specific class of problems. Linear and non-linear numerical experiments reveal that our new approach leads to faster convergence than existing state-of-the-art preconditioners for a broader range of problems than indicated by the theory alone. We present a range of numerical experiments performed in serial, with further improvements expected if the highly parallelisable nature of the preconditioners is exploited.

1 Introduction

Data assimilation has seen substantial research interest in fields including numerical weather prediction [6, 29], ecology [27, 28] and hydrology [7, 39] in recent decades. The variational data assimilation problem can be written mathematically as follows: For a given time window $[t_0, t_N]$, let $\mathbf{x}_i^t \in \mathbb{R}^s$ be the true state of a dynamical system of interest at time t_i , where s is the number of state variables. Data assimilation algorithms combine observations of a dynamical system, $\mathbf{y}_i \in \mathbb{R}^{p_i}$ at times t_i , with prior information from a model, $\mathbf{x}_b \in \mathbb{R}^s$, to find $\mathbf{x}_i \in \mathbb{R}^s$, the most likely state of the system at time t_i . The prior, or background state, is valid at the initial time t_0 and can be written as an approximation to the true state via $\mathbf{x}_b = \mathbf{x}_0^t + \epsilon^b$. We assume that the background errors $\epsilon^b \sim \mathcal{N}(0, \mathbf{B})$, where $\mathbf{B} \in \mathbb{R}^{s \times s}$ is the background error covariance matrix. In order to compare observations made at different locations, or of different variables to those in the state vector \mathbf{x}_i , we define a, possibly non-linear, observation operator $\mathcal{H}_i : \mathbb{R}^s \rightarrow \mathbb{R}^{p_i}$ which maps from state variable space to observation space at time t_i . Observations $\mathbf{y}_i \in \mathbb{R}^{p_i}$ at time t_i are written as $\mathbf{y}_i = \mathcal{H}_i[\mathbf{x}_i^t] + \epsilon_i$ for $i = 0, \dots, N$, where the observation error $\epsilon_i \sim \mathcal{N}(0, \mathbf{R}_i)$ and $\mathbf{R}_i \in \mathbb{R}^{p_i \times p_i}$ are the observation error covariance (OEC) matrices.

In weak-constraint four-dimensional variational data assimilation (4D-Var) the state \mathbf{x}_{i-1} at time t_{i-1} is propagated to the next observation time t_i using an imperfect forecast model, \mathcal{M}_i , to obtain $\mathbf{x}_i = \mathcal{M}_i(\mathbf{x}_{i-1}) + \epsilon_i^m$. The model error at each time is given by $\epsilon_i^m \sim \mathcal{N}(0, \mathbf{Q}_i)$, where $\mathbf{Q}_i \in \mathbb{R}^{s \times s}$ is the model error covariance matrix at time t_i . It is typically assumed that the error covariance matrices are mutually uncorrelated across different types and different observation times. The analysis, or most likely state \mathbf{x}_0 at time t_0 , minimises the weak constraint 4D-Var objective function

given by

$$J(\mathbf{x}_0) = (\mathbf{x}_0 - \mathbf{x}_b)^\top \mathbf{B}^{-1} (\mathbf{x}_0 - \mathbf{x}_b) + \sum_{i=0}^N (\mathbf{y}_i - \mathcal{H}_i[\mathbf{x}_i])^\top \mathbf{R}_i^{-1} (\mathbf{y}_i - \mathcal{H}_i[\mathbf{x}_i]) + \sum_{i=1}^N (\mathbf{x}_i - \mathcal{M}_i(\mathbf{x}_{i-1}))^\top \mathbf{Q}_i^{-1} (\mathbf{x}_i - \mathcal{M}_i(\mathbf{x}_{i-1})). \quad (1)$$

Weak-constraint 4D-Var is used in numerical weather prediction (NWP) to estimate the initial condition for a weather forecast [37, 38]. Practical implementations of (1) pose mathematical and computational challenges. Firstly, the dimension of the problem can be large; in NWP [6] the dimension of the state can be of order 10^9 ,

and the number of observations can be of order 10^6 . This application is also time critical, so the time that can be allocated to the data assimilation procedure is very limited in operational situations. Computational efficiency is therefore vital, and designing techniques to ensure fast convergence of the minimisation of the objective function has been an ongoing area of research interest, see for instance [13, 5, 9, 19].

The weak constraint objective function (1) is typically solved via an incremental approach, where a small number of nonlinear outer loops and a larger number of linearised inner loops are solved [16, 17]. Standard Krylov subspace solvers can then be applied for the inner loops. An alternative approach involves solving the linearised inner loop using a saddle point formulation [15, 13, 18, 8]. This has increased potential for parallelisation, which can allow full exploitation of modern computer architectures. Prior work has considered the development of specific preconditioners for the saddle point data assimilation problem [15, 13], typically focusing on approximations to the term containing information about the linearised model. Block diagonal preconditioners are appealing, due to the potential to apply the MINRES algorithm and develop guaranteed theoretical insight about the convergence rates based on the eigenvalues of the preconditioned system, although inexact constraint preconditioners with GMRES have been found to yield better performance in data assimilation settings for a variety of problems [15, 14].

However, previous research on the primal form of the variational data assimilation problem has revealed that the observation error covariance matrices \mathbf{R}_i play an important role in determining the convergence of iterative methods [34, 35]. In the last decade, researchers have increasingly made use of observing systems that have correlated observation error covariance matrices [40, 33]. Previous saddle point preconditioners typically apply the exact inverses of \mathbf{R}_i [15, 18], which is known to be computationally infeasible for many satellite observing systems [40, 36]. It is therefore expected that new terms within saddle point preconditioners which incorporate correlated information from \mathbf{R}_i and are inexpensive to apply could be beneficial in terms of convergence and wallclock speed.

In this paper, we propose new preconditioning approaches for the model and observation terms within the saddle point framework. In particular we propose a number of approaches which have the additional benefit of being highly parallelisable. To our knowledge our preconditioners account explicitly for model information within the model term for the first time. We begin in Section 2 by introducing the saddle point formulation of the weak-constraint 4D-Var data assimilation problem, and presenting existing state-of-the-art preconditioners for the saddle point setting. In Section 3 we prove bounds on the eigenvalues of a block diagonal preconditioned system in terms of constituent matrices of the saddle point problem. In Sections 4 and 5 we then analyse the effect of applying existing and new preconditioners for the model term and observation error covariance term respectively. In Section 6 we present two numerical set-ups of interest, and investigate how the conclusions of the previous sections apply in linear and non-linear settings. The experimental results for a linear and non-linear model are presented in Section 7. For the heat equation, where the simplifying theoretical assumptions of Section 4 are satisfied, we find that our new preconditioners result in superior performance than state-of-the-art block diagonal and inexact constraint preconditioners in a variety of settings. For the nonlinear Lorenz 96 problem, the assumptions of Section 4 are not satisfied, however our new approaches remain beneficial for the inexact constraint preconditioner. We note that all of the experiments presented in this paper are performed in serial, as the goal of this paper is not to suggest a cutting-edge parallel implementation, but rather justify novel preconditioners which can be applied in this setting. Incorporating these preconditioning strategies into a parallel implementation is expected to result in further significant improvements in wallclock time. Finally, in Section 8 we present our conclusions.

2 Background

2.1 Data assimilation

In this section we introduce the saddle point formulation of the weak constraint four-dimensional variational (4D-Var) data assimilation problem (1). Given a time window $[t_0, t_N]$, split into N subwindows, we wish to find the state $\mathbf{x} \in \mathbb{R}^s$ at time t_0 , that is closest in a weighted norm sense both to the observations throughout the time window and to prior information at the initial time propagated by a model. The incremental primal formulation updates $\mathbf{x}_0^{(l+1)} = \mathbf{x}_0^{(l)} + \delta\mathbf{x}^{(l)}$ by solving an objective function via a series of inner and outer loops to find a sequence of increments to the background state $\mathbf{x}_b = \mathbf{x}_0^{(0)}$. In the inner loop a linearised problem is solved, typically using iterative solvers such as the Conjugate Gradient method [21], and the outer loop is used to update linearisations of model and observation operators.

For each outer loop l , the inner loop minimises a quadratic objective function to find $\delta\mathbf{x}^{(l)} \in \mathbb{R}^s$. The full non-linear observation operator \mathcal{H}_i (similarly the model operator \mathcal{M}_i) is linearised about the current best guess

$\mathbf{x}_0^{(l)}$ to obtain the linearised operator $\mathbf{H}_i^{(l)}$ (respectively $\mathbf{M}_i^{(l)}$). The updated initial guess $\delta\mathbf{x}_0^{(l)}$ is propagated forward between observation times by $\mathbf{M}_i^{(l)}$ to obtain $\delta\mathbf{x}_{i+1}^{(l)} = \mathbf{M}_i^{(l)}\delta\mathbf{x}_i^{(l)}$. We note that the time between observations is likely to consist of multiple numerical model time-steps, hence $\mathbf{M}_i^{(l)}$ often corresponds to the composition of many discretised models for a single observation time-step.

Alternatively, the quadratic objective function in the inner loop may be replaced with a saddle point system. Following the notation of [18, Eq. (2.5)], we substitute the linearised objective function with the following saddle point system:

$$\begin{pmatrix} \mathbf{D} & \mathbf{0} & \mathbf{L} \\ \mathbf{0} & \mathbf{R} & \mathbf{H} \\ \mathbf{L}^\top & \mathbf{H}^\top & \mathbf{0} \end{pmatrix} \begin{pmatrix} \delta\boldsymbol{\eta} \\ \delta\boldsymbol{\nu} \\ \delta\mathbf{x} \end{pmatrix} = \begin{pmatrix} \mathbf{b} \\ \mathbf{d} \\ \mathbf{0} \end{pmatrix}. \quad (2)$$

In this paper we focus on new preconditioners to the saddle point coefficient matrix:

$$\mathcal{A} = \begin{pmatrix} \mathbf{D} & \mathbf{0} & \mathbf{L} \\ \mathbf{0} & \mathbf{R} & \mathbf{H} \\ \mathbf{L}^\top & \mathbf{H}^\top & \mathbf{0} \end{pmatrix} \in \mathbb{R}^{(2s+p)(N+1) \times (2s+p)(N+1)}, \quad (3)$$

where \mathbf{D} , \mathbf{R} , \mathbf{H} are the following block diagonal matrices:

$$\begin{aligned} \mathbf{D} &= \text{blkdiag}(\mathbf{B}, \mathbf{Q}_1, \mathbf{Q}_2, \dots, \mathbf{Q}_N) \in \mathbb{R}^{(N+1)s \times (N+1)s}, \\ \mathbf{R} &= \text{blkdiag}(\mathbf{R}_0, \mathbf{R}_1, \mathbf{R}_2, \dots, \mathbf{R}_N) \in \mathbb{R}^{(N+1)p \times (N+1)p}, \\ \mathbf{H} &= \text{blkdiag}(\mathbf{H}_0^{(l)}, \mathbf{H}_1^{(l)}, \mathbf{H}_2^{(l)}, \dots, \mathbf{H}_N^{(l)}) \in \mathbb{R}^{(N+1)s \times (N+1)s}, \end{aligned}$$

with the i th block in each case being the relevant matrix for time t_i . Here, the MATLAB-style notation ‘`blkdiag`’ is used to describe a block diagonal matrix in terms of its block diagonal entries.

We note that for non-linear models \mathcal{M}_i (respectively observation operators \mathcal{H}_i) the adjoint model $(\mathbf{M}_i^{(l)})^{AD}$ (respectively $(\mathbf{H}_i^{(l)})^{AD}$) is typically not equal to the transpose of the linearised forward model, or tangent linear model, i.e. $(\mathbf{M}_i^{(l)})^\top \neq (\mathbf{M}_i^{(l)})^{AD}$ (respectively $(\mathbf{H}_i^{(l)})^\top \neq (\mathbf{H}_i^{(l)})^{AD}$). This means that the coefficient matrix \mathcal{A} may not be symmetric. We write \mathcal{A} in the form (3) for the linear case, and for the non-linear setting we employ the notation \mathbf{L}^\top and \mathbf{H}^\top in the sense of adjoint operators rather than necessarily symmetric matrices.

The matrix \mathbf{L} contains the linearised model information that evolves \mathbf{x}_0 throughout the N subwindows, written

$$\mathbf{L} = \begin{pmatrix} \mathbf{I} & & & & & \\ -\mathbf{M}_1^{(l)} & \mathbf{I} & & & & \\ & -\mathbf{M}_2^{(l)} & \mathbf{I} & & & \\ & & \ddots & \ddots & & \\ & & & & \ddots & \\ & & & & & -\mathbf{M}_N^{(l)} & \mathbf{I} \end{pmatrix}, \quad (4)$$

where \mathbf{I} denotes the $s \times s$ identity matrix. As we consider preconditioners for the inner loop only, for the remainder of the paper we drop the superscripts that denote the outer loop iteration, and simply use \mathbf{H}_i and \mathbf{M}_i .

The saddle point system is expected to be useful for data assimilation systems as it is much more parallelisable than the primal form [15]. Therefore, it is more amenable to methods for modern computer architectures. This is particularly important as rapid convergence of the data assimilation step is vital for numerical weather prediction systems, and other operational implementations. As the saddle point system is indefinite, methods such as the Conjugate Gradient algorithm cannot be used. Depending on the choice of preconditioner, MINRES [26] or GMRES [32] are examples of viable algorithms for solving linear systems of the form (2).

Numerical methods for saddle point systems are well-studied in the optimisation literature (see [1] for a comprehensive survey). In order to devise suitable approximations of such systems, as in the forthcoming section, one powerful approach is to approximate the ‘leading’ (1,1) block of the matrix, along with its Schur complement [23, 25]. For saddle point problems arising from data assimilation, not only does the (1,1) block often have complex structure, but the constraint block contains evolution of the model terms forward/backward in time leading to a Schur complement which is very difficult to cheaply approximate [13]. Therefore, approximating the constraint block cheaply is an important consideration for a good preconditioner of the matrix (3). The work presented here

provide value. However, we consider preconditioners for the first outer loop where there is no additional information, and hence developing computationally feasible stand-alone preconditioners is crucial.

In most prior work the exact observation error covariance matrix has been used in preconditioners. This is due to the fact that the cost of applying \mathbf{R}^{-1} is assumed not to be prohibitive, due to the inherent block diagonal structure of \mathbf{R} . However, the rising use of more complex correlation structures (such as inter-channel observation errors, see [40]) means that applying \mathbf{R}^{-1} exactly is not always affordable and may be a computational bottleneck. One option is to apply a computationally cheap approximation of \mathbf{R} within the preconditioner, such as the diagonal of \mathbf{R} , however this is typically an inaccurate approximation which can significantly delay convergence. In this paper we consider new classes of preconditioner for the observation error covariance term.

3 Bounds on eigenvalues for the block diagonal preconditioner

For a block diagonal preconditioner of the form \mathcal{P}_D , it is possible to describe the convergence of the preconditioned MINRES algorithm by analysing the eigenvalues of the preconditioned system (see [11, Chapter 4], for instance). The matrices \mathcal{A} and \mathcal{P}_D defined in (3) and (5) can be written as

$$\mathcal{A} = \begin{pmatrix} \Phi & \Psi^\top \\ \Psi & \mathbf{0} \end{pmatrix}, \quad \mathcal{P}_D = \begin{pmatrix} \hat{\Phi} & \mathbf{0} \\ \mathbf{0} & \hat{\mathbf{S}} \end{pmatrix}, \quad (6)$$

where

$$\Phi = \begin{pmatrix} \mathbf{D} & \mathbf{0} \\ \mathbf{0} & \mathbf{R} \end{pmatrix}, \quad \Psi = \begin{pmatrix} \mathbf{L}^\top & \mathbf{H}^\top \end{pmatrix},$$

and with $\hat{\Phi}$ and $\hat{\mathbf{S}}$ approximations of Φ and the (negative) Schur complement $\mathbf{S} = \Psi\Phi^{-1}\Psi^\top$.

We now denote

$$\tilde{\mathbf{S}} = \mathbf{L}^\top \mathbf{D}^{-1} \mathbf{L}, \quad \hat{\mathbf{S}} = \hat{\mathbf{L}}^\top \mathbf{D}^{-1} \hat{\mathbf{L}},$$

where $\hat{\mathbf{D}}$, $\hat{\mathbf{R}}$, $\hat{\mathbf{L}}$ are approximations of \mathbf{D} , \mathbf{R} , \mathbf{L} . For the forthcoming theory, we suppose that \mathbf{D} , $\hat{\mathbf{D}}$, \mathbf{R} , $\hat{\mathbf{R}}$, \mathbf{S} , $\tilde{\mathbf{S}}$, $\hat{\mathbf{S}}$ are symmetric positive definite, with

$$\lambda(\hat{\mathbf{D}}^{-1}\mathbf{D}) \in [\lambda_{\mathbf{D}}, \Lambda_{\mathbf{D}}], \quad \lambda(\hat{\mathbf{R}}^{-1}\mathbf{R}) \in [\lambda_{\mathbf{R}}, \Lambda_{\mathbf{R}}], \quad \lambda(\tilde{\mathbf{S}}^{-1}\mathbf{S}) \in [\lambda_{\mathbf{S}}, \Lambda_{\mathbf{S}}], \quad \lambda\left((\hat{\mathbf{L}}^\top \hat{\mathbf{L}})^{-1}(\mathbf{L}^\top \mathbf{L})\right) \in [\lambda_{\mathbf{L}}, \Lambda_{\mathbf{L}}],$$

where $\lambda(\cdot)$ denotes the eigenvalues of a matrix. We may then prove the following result:

Theorem 1. *With the definitions as stated above, the eigenvalues of $\mathcal{P}_D^{-1}\mathcal{A}$ are real, and satisfy:*

$$\lambda(\mathcal{P}_D^{-1}\mathcal{A}) \in \left[\frac{\lambda_{\Phi} - \sqrt{\lambda_{\Phi}^2 + 4\Lambda_{\Phi}\Lambda_{\mathbf{S}}\Lambda_{\mathbf{L}}\kappa(\mathbf{D})}}{2}, \frac{\Lambda_{\Phi} - \sqrt{\Lambda_{\Phi}^2 + \frac{4\lambda_{\Phi}\lambda_{\mathbf{S}}\lambda_{\mathbf{L}}}{\kappa(\mathbf{D})}}}{2} \right] \\ \cup [\lambda_{\Phi}, \Lambda_{\Phi}] \cup \left[\frac{\lambda_{\Phi} + \sqrt{\lambda_{\Phi}^2 + \frac{4\lambda_{\Phi}\lambda_{\mathbf{S}}\lambda_{\mathbf{L}}}{\kappa(\mathbf{D})}}}{2}, \frac{\Lambda_{\Phi} + \sqrt{\Lambda_{\Phi}^2 + 4\Lambda_{\Phi}\Lambda_{\mathbf{S}}\Lambda_{\mathbf{L}}\kappa(\mathbf{D})}}{2} \right],$$

where $\lambda_{\Phi} = \min\{\lambda_{\mathbf{D}}, \lambda_{\mathbf{R}}\}$, $\Lambda_{\Phi} = \max\{\Lambda_{\mathbf{D}}, \Lambda_{\mathbf{R}}\}$, and $\kappa(\cdot)$ denotes the condition number of a matrix.

Proof. Applying well-known results (see [31, p. 2906], [30, Theorem 4.2.1]), we have that

$$\lambda \in \left[\frac{\delta - \sqrt{\delta^2 + 4\Delta\Phi}}{2}, \frac{\Delta - \sqrt{\Delta^2 + 4\delta\phi}}{2} \right] \cup [\delta, \Delta] \cup \left[\frac{\delta + \sqrt{\delta^2 + 4\delta\phi}}{2}, \frac{\Delta + \sqrt{\Delta^2 + 4\Delta\Phi}}{2} \right], \quad (7)$$

where δ , ϕ denote the minimum eigenvalues of $\hat{\Phi}^{-1}\Phi$, $\hat{\mathbf{S}}^{-1}\mathbf{S}$ for a general block diagonal saddle point preconditioner (6), and Δ , Φ represent the corresponding maximum eigenvalues.

Clearly, for this problem $\delta = \lambda_{\Phi}$ and $\Delta = \Lambda_{\Phi}$. It remains to analyse the minimum and maximum eigenvalues of the preconditioned Schur complement, which we note is within the range of the Rayleigh quotient (for $\mathbf{x} \neq \mathbf{0}$):

$$\frac{\mathbf{x}^\top \mathbf{S} \mathbf{x}}{\mathbf{x}^\top \hat{\mathbf{S}} \mathbf{x}} = \frac{\mathbf{x}^\top \mathbf{S} \mathbf{x}}{\mathbf{x}^\top \hat{\mathbf{S}} \mathbf{x}} \cdot \frac{\mathbf{x}^\top \tilde{\mathbf{S}} \mathbf{x}}{\mathbf{x}^\top \tilde{\mathbf{S}} \mathbf{x}} = \frac{\mathbf{x}^\top \mathbf{S} \mathbf{x}}{\mathbf{x}^\top \tilde{\mathbf{S}} \mathbf{x}} \cdot \frac{\mathbf{x}^\top \mathbf{L}^\top \mathbf{D}^{-1} \mathbf{L} \mathbf{x}}{\mathbf{x}^\top \mathbf{L}^\top \mathbf{L} \mathbf{x}} \cdot \frac{\mathbf{x}^\top \mathbf{L}^\top \mathbf{L} \mathbf{x}}{\mathbf{x}^\top \hat{\mathbf{L}}^\top \hat{\mathbf{L}} \mathbf{x}} \cdot \frac{\mathbf{x}^\top \hat{\mathbf{L}}^\top \hat{\mathbf{L}} \mathbf{x}}{\mathbf{x}^\top \hat{\mathbf{L}}^\top \mathbf{D}^{-1} \hat{\mathbf{L}} \mathbf{x}}. \quad (8)$$

Observing that

$$\begin{aligned} \frac{\mathbf{x}^\top \mathbf{S} \mathbf{x}}{\mathbf{x}^\top \tilde{\mathbf{S}} \mathbf{x}} &\in [\lambda_{\mathbf{S}}, \Lambda_{\mathbf{S}}], & \frac{\mathbf{x}^\top \mathbf{L}^\top \mathbf{D}^{-1} \mathbf{L} \mathbf{x}}{\mathbf{x}^\top \mathbf{L}^\top \mathbf{L} \mathbf{x}} &= \frac{\mathbf{y}^\top \mathbf{y}}{\mathbf{y}^\top \mathbf{D} \mathbf{y}} \in \left[\frac{1}{\Lambda_{\mathbf{D}}}, \frac{1}{\lambda_{\mathbf{D}}} \right], \\ \frac{\mathbf{x}^\top \mathbf{L}^\top \mathbf{L} \mathbf{x}}{\mathbf{x}^\top \widehat{\mathbf{L}}^\top \widehat{\mathbf{L}} \mathbf{x}} &\in [\lambda_{\mathbf{L}}, \Lambda_{\mathbf{L}}], & \frac{\mathbf{x}^\top \widehat{\mathbf{L}}^\top \widehat{\mathbf{L}} \mathbf{x}}{\mathbf{x}^\top \widehat{\mathbf{L}}^\top \mathbf{D}^{-1} \widehat{\mathbf{L}} \mathbf{x}} &= \frac{\mathbf{z}^\top \mathbf{D} \mathbf{z}}{\mathbf{z}^\top \mathbf{z}} \in [\lambda_{\mathbf{D}}, \Lambda_{\mathbf{D}}], \end{aligned}$$

where $\mathbf{y} = \mathbf{D}^{-1/2} \mathbf{L} \mathbf{x} \neq \mathbf{0}$, $\mathbf{z} = \mathbf{D}^{-1/2} \widehat{\mathbf{L}} \mathbf{x} \neq \mathbf{0}$, we may write that

$$\frac{\mathbf{x}^\top \mathbf{S} \mathbf{x}}{\mathbf{x}^\top \widehat{\mathbf{S}} \mathbf{x}} \in \left[\frac{\lambda_{\mathbf{S}} \lambda_{\mathbf{D}} \lambda_{\mathbf{L}}}{\Lambda_{\mathbf{D}}}, \frac{\Lambda_{\mathbf{S}} \Lambda_{\mathbf{D}} \Lambda_{\mathbf{L}}}{\lambda_{\mathbf{D}}} \right] = \left[\frac{\lambda_{\mathbf{S}} \lambda_{\mathbf{L}}}{\kappa(\mathbf{D})}, \Lambda_{\mathbf{S}} \Lambda_{\mathbf{L}} \kappa(\mathbf{D}) \right].$$

Therefore, it holds that $\phi \geq \frac{\lambda_{\mathbf{S}} \lambda_{\mathbf{L}}}{\kappa(\mathbf{D})}$ and $\Phi \leq \Lambda_{\mathbf{S}} \Lambda_{\mathbf{L}} \kappa(\mathbf{D})$. Substituting the bounds for δ , Δ , ϕ , Φ into (7) then gives the result. \square

Remark. *Due to the way the Rayleigh quotient is factored in (8), Theorem 1 gives a potentially very weak bound when \mathbf{D} is ill-conditioned. We find the main features which affect the quality of the preconditioner, as predicted by the result, are the approximations of \mathbf{D} and \mathbf{R} , the effect of dropping the second term of the Schur complement, and the quality of the approximation of $\mathbf{L}^\top \mathbf{L}$ (characterised by the eigenvalues of $\widehat{\mathbf{L}}^{-\top} \mathbf{L}^\top \mathbf{L} \widehat{\mathbf{L}}^{-1}$). The latter quantity is the subject of the forthcoming analysis.*

4 Approximating $\widehat{\mathbf{L}}$

Theorem 1 suggests that the eigenvalues of the preconditioned system are highly influenced by the quality of the approximation of $\widehat{\mathbf{L}}^\top \widehat{\mathbf{L}}$ to $\mathbf{L}^\top \mathbf{L}$ in the block diagonal preconditioner. In this section we consider existing and new choices of $\widehat{\mathbf{L}}$. In particular we analyse the eigenvalues and structure of $\widehat{\mathbf{L}}^{-\top} \mathbf{L}^\top \mathbf{L} \widehat{\mathbf{L}}^{-1}$, similar to $(\widehat{\mathbf{L}}^\top \widehat{\mathbf{L}})^{-1} (\mathbf{L}^\top \mathbf{L})$, for two choices of $\widehat{\mathbf{L}}$. The first choice of $\widehat{\mathbf{L}}$, \mathbf{L}_0 has previously been used for saddle point preconditioners for the data assimilation problem [15, 18]. We also propose \mathbf{L}_M , a new class of preconditioners that depends on a user-defined parameter and incorporates model information while guaranteeing parallelisability of $\widehat{\mathbf{L}}$ and its inverse.

For \mathbf{L}_M , the user selects an integer value of k , and every k th block (i.e. $\mathbf{M}_k, \mathbf{M}_{2k}, \mathbf{M}_{3k}, \dots$) is set equal to $\mathbf{0}$. The other entries of \mathbf{L}_M correspond to those of \mathbf{L} . Formally we write this as in the definition below.

Definition 1. *Let $k \in \mathbb{N}$, and let $\mathbf{L}_M = \mathbf{L}_M(k) \in \mathbb{R}^{(N+1)s \times (N+1)s}$ be a block matrix made up of $s \times s$ blocks. For $i, j = 1, \dots, N+1$ we define*

$$\text{the } (i, j)\text{th block of } \mathbf{L}_M = \begin{cases} \mathbf{I} & \text{if } i = j, \\ -\mathbf{M}_j & \text{if } i = j + 1 \text{ and } j \text{ is not divisible by } k, \\ \mathbf{0} & \text{otherwise.} \end{cases}$$

Similarly we can write the inverse of \mathbf{L}_M as follows:

Definition 2. *Let $k \in \mathbb{N}$, and let $\mathbf{L}_M = \mathbf{L}_M(k) \in \mathbb{R}^{(N+1)s \times (N+1)s}$ be a block matrix made up of $s \times s$ blocks. For $i, j = 1, \dots, N+1$ we define*

$$\text{the } (i, j)\text{th block of } \mathbf{L}_M^{-1} = \begin{cases} \mathbf{I} & \text{if } i = j, \\ \prod_{m=1}^{j-i} \mathbf{M}_{i-m} & \text{if } 1 \leq i - j \leq (i - 1) \bmod(k), \\ \mathbf{0} & \text{otherwise.} \end{cases}$$

We note that the number of terms in the products of \mathbf{L}_M^{-1} are controlled by the parameter k , and that \mathbf{L}_M^{-1} is block lower triangular. Note that \mathbf{L} , defined in (4), satisfies $\mathbf{L} = \mathbf{L}_M(N+1)$ according to this notation. Further, the choice $k = 1$ corresponds to $\mathbf{L}_M(1) = \mathbf{L}_0 = \mathbf{I}$. The structure of the approximation \mathbf{L}_M means that, unlike \mathbf{L} itself, its inverse operation may be trivially parallelised, and run on up to $\lceil \frac{N+1}{k} \rceil$ processors. For smaller values of k , multiplication by \mathbf{L}_M^{-1} also incorporates important model information. To further justify the effectiveness of this approximation, we study the eigenvalues of $\mathbf{L}_M^{-\top} \mathbf{L}^\top \mathbf{L} \mathbf{L}_M^{-1}$ theoretically in Section 4.2.

4.1 Eigenvalues of $\mathbf{L}^\top \mathbf{L}$

In this section we consider the eigenvalues of the unpreconditioned model term. We recall that as $\mathbf{L}_0 = \mathbf{I}$ these bounds also apply to the standard ‘preconditioning’ with \mathbf{L}_0 .

Assumption. Let $\mathbf{M}_i \equiv \mathbf{M} \forall i \in \{1, 2, \dots, N\}$, where $\mathbf{M} \in \mathbb{R}^{s \times s}$ is symmetric.

Lemma 1. $\mathbf{L}^\top \mathbf{L}$ is positive definite by construction.

Proof. By [42, Theorem 7.3] $\mathbf{L}^\top \mathbf{L}$ is positive semi-definite. Clearly \mathbf{L} is full rank, hence the product $\mathbf{L}^\top \mathbf{L}$ is strictly positive definite. \square

Further, for any symmetric choice of \mathbf{M} we can bound the eigenvalues of $\mathbf{L}^\top \mathbf{L}$ above in terms of those of \mathbf{M} .

Proposition 1. Let \mathbf{M} be symmetric with eigenvalues in $\gamma \leq \lambda(\mathbf{M}) \leq \mu$. Then the eigenvalues of $\mathbf{L}^\top \mathbf{L}$ are bounded above by

$$\lambda(\mathbf{L}^\top \mathbf{L}) \leq 1 + \max\{\mu^2, \gamma^2\} + \max\{2|\gamma|, 2|\mu|\} = (1 + \max\{|\mu|, |\gamma|\})^2. \quad (9)$$

Proof. We begin by proving the upper bound. We decompose $\mathbf{L}^\top \mathbf{L}$ as the sum of the identity, a block diagonal matrix and a Kronecker product:

$$\begin{aligned} \mathbf{L}^\top \mathbf{L} &= \mathbf{I} + \text{diag}(\mathbf{M}^2, \mathbf{M}^2, \dots, \mathbf{M}^2, \mathbf{0}) + \text{tridiag}(-\mathbf{M}, \mathbf{0}, -\mathbf{M}) \\ &= \mathbf{I} + \text{diag}(\mathbf{M}^2, \mathbf{M}^2, \dots, \mathbf{M}^2, \mathbf{0}) + \text{tridiag}(1, 0, 1) \otimes (-\mathbf{M}), \end{aligned} \quad (10)$$

where tridiag denotes a (block) tridiagonal matrix given the (block) sub-diagonal, diagonal, and super-diagonal entries all the same and as specified in turn. As all matrices being considered are symmetric, using [4, Fact 5.12.2] we can bound the maximum eigenvalue above by

$$\lambda_{\max}(\mathbf{L}^\top \mathbf{L}) \leq 1 + \lambda_{\max}(\text{diag}(\mathbf{M}^2, \mathbf{M}^2, \dots, \mathbf{M}^2, \mathbf{0})) + \lambda_{\max}(\text{tridiag}(1, 0, 1) \otimes (-\mathbf{M})).$$

The largest eigenvalue of $\text{diag}(\mathbf{M}^2, \mathbf{M}^2, \dots, \mathbf{M}^2, \mathbf{0})$ is given by $\max\{\gamma^2, \mu^2\}$.

By [22, Theorem 4.2.12] the eigenvalues of a Kronecker product are given by the product of the eigenvalues of the individual matrices. The eigenvalues of $-\mathbf{M}$ are contained in the range $-\mu \leq \lambda(-\mathbf{M}) \leq -\gamma$. The eigenvalues of $\text{tridiag}(1, 0, 1)$ are given by:

$$\lambda(\text{tridiag}(1, 0, 1)) = -2 \cos\left(\frac{k\pi}{N+2}\right), \quad k = 1, \dots, N+1.$$

Therefore $-2 < \lambda(\text{tridiag}(1, 0, 1)) < 2$. This means the largest eigenvalue of $\text{tridiag}(1, 0, 1) \otimes (-\mathbf{M})$ is strictly bounded above by $\max\{2|\mu|, 2|\gamma|\}$. Substituting this into (10) and rearranging yields the upper bound of (9). \square

Under the additional assumption that \mathbf{M} is positive semi-definite we can obtain a positive lower bound for the smallest eigenvalue of $\mathbf{L}^\top \mathbf{L}$, as shown below.

Proposition 2. Let \mathbf{M} be symmetric and positive semi-definite with $\lambda_{\max}(\mathbf{M}) = \mu \leq 1$. We can bound the eigenvalues of $\mathbf{L}^\top \mathbf{L}$ below by

$$\lambda(\mathbf{L}^\top \mathbf{L}) \geq (1 - \mu)^2.$$

Proof. We begin by considering $\mathbf{v}^\top \mathbf{L}^\top \mathbf{L} \mathbf{v}$. This can be expanded as

$$\mathbf{v}^\top \mathbf{L}^\top \mathbf{L} \mathbf{v} = \mathbf{v}^\top \mathbf{v} + \sum_{i=1}^N [-2\mathbf{v}_i^\top \mathbf{M} \mathbf{v}_{i+1} + \mathbf{v}_i^\top \mathbf{M}^2 \mathbf{v}_i].$$

Using the Cauchy–Schwarz inequality we can bound $\mathbf{v}_i^\top \mathbf{M} \mathbf{v}_{i+1}$ above by

$$\mathbf{v}_i^\top \mathbf{M} \mathbf{v}_{i+1} \leq |\mathbf{v}_i^\top \mathbf{M} \mathbf{v}_i|^{1/2} |\mathbf{v}_{i+1}^\top \mathbf{M} \mathbf{v}_{i+1}|^{1/2}$$

As the algebraic relation $-2\sqrt{|a||b|} \geq -|a| - |b|$ holds¹, this allows us to bound $\mathbf{v}^\top \mathbf{L}^\top \mathbf{L} \mathbf{v}$ below by

$$\begin{aligned} \mathbf{v}^\top \mathbf{L}^\top \mathbf{L} \mathbf{v} &\geq \sum_{i=1}^{N+1} \mathbf{v}_i^\top \mathbf{I} \mathbf{v}_i + \sum_{i=1}^N [\mathbf{v}_i^\top \mathbf{M}^2 \mathbf{v}_i - |\mathbf{v}_i^\top \mathbf{M} \mathbf{v}_i| - |\mathbf{v}_{i+1}^\top \mathbf{M} \mathbf{v}_{i+1}|] \\ &\geq \sum_{i=2}^N \mathbf{v}_i (\mathbf{I} + \mathbf{M}^2 - 2\mathbf{M}) \mathbf{v}_i + \mathbf{v}_1^\top \mathbf{I} \mathbf{v}_1 + \mathbf{v}_1^\top \mathbf{M}^2 \mathbf{v}_1 - \mathbf{v}_1^\top \mathbf{M} \mathbf{v}_1 + \mathbf{v}_{N+1}^\top \mathbf{v}_{N+1} - \mathbf{v}_{N+1}^\top \mathbf{M} \mathbf{v}_{N+1}. \end{aligned}$$

As \mathbf{M} is positive semi-definite, we can subtract $\mathbf{v}_1^\top \mathbf{M} \mathbf{v}_1$ from the lower bound, which yields

$$\mathbf{v}^\top \mathbf{L}^\top \mathbf{L} \mathbf{v} \geq \mathbf{v}_{N+1}^\top \mathbf{I} \mathbf{v}_{N+1} - \mathbf{v}_{N+1}^\top \mathbf{M} \mathbf{v}_{N+1} + \sum_{i=1}^N \mathbf{v}_i (\mathbf{I} + \mathbf{M}^2 - 2\mathbf{M}) \mathbf{v}_i.$$

By the assumption that $\lambda_{\max}(\mathbf{M}) = \mu \leq 1$, we can reason that $\mathbf{M} - \mathbf{M}^2$ is positive semi-definite. Therefore we can also subtract $\mathbf{v}_{N+1}^\top (\mathbf{M} - \mathbf{M}^2) \mathbf{v}_{N+1}$ (a positive quantity) from the lower bound to obtain

$$\mathbf{v}^\top \mathbf{L}^\top \mathbf{L} \mathbf{v} \geq \sum_{i=1}^{N+1} \mathbf{v}_i (\mathbf{I} + \mathbf{M}^2 - 2\mathbf{M}) \mathbf{v}_i.$$

This can be viewed as a scaled Rayleigh quotient, for a block diagonal matrix with $\mathbf{I} + \mathbf{M}^2 - 2\mathbf{M}$ on each of the blocks. The Rayleigh quotient is bounded below by the minimum eigenvalue of the matrix. Therefore

$$\frac{\mathbf{v}^\top \mathbf{L}^\top \mathbf{L} \mathbf{v}}{\mathbf{v}^\top \mathbf{v}} \geq \lambda_{\min}(\mathbf{I} + \mathbf{M}^2 - 2\mathbf{M}) = \lambda_{\min}((\mathbf{I} - \mathbf{M})^2) = (1 - \lambda_{\max}(\mathbf{M}))^2 = (1 - \mu)^2,$$

as required. The last equality follows due to the fact that $\lambda_{\max}(\mathbf{M}) = \mu \leq 1$. \square

4.2 Eigenvalues of $\mathbf{L}_M^{-\top} \mathbf{L}^\top \mathbf{L} \mathbf{L}_M^{-1}$

We now consider the eigenvalues of the preconditioned model term, using the new preconditioner \mathbf{L}_M . We begin by considering a general choice of k , and later develop specific bounds for $k = 3$ and $k = 4$.

Theorem 2. *Let \mathbf{L} be defined as in (4) and \mathbf{L}_M in Definition 1 with $\mathbf{M}_i \equiv \mathbf{M}$ for all subwindows i , where \mathbf{M} is symmetric. The eigenvalues of $\mathbf{L}_M^{-\top} \mathbf{L}^\top \mathbf{L} \mathbf{L}_M^{-1}$ can be computed in terms of the eigenvalues of \mathbf{M} for any choice of k .*

Proof. We begin by writing

$$\mathbf{L}_M^{-\top} \mathbf{L}^\top \mathbf{L} \mathbf{L}_M^{-1} = \mathbf{I} + \mathbf{A}(\mathbf{M}), \quad (11)$$

where \mathbf{A} is a matrix consisting entirely of blocks of zeros and powers of \mathbf{M} .

The eigenvalues of (11) are given by

$$\lambda(\mathbf{L}_M^{-\top} \mathbf{L}^\top \mathbf{L} \mathbf{L}_M^{-1}) = 1 + \lambda(\mathbf{A}(\mathbf{M})).$$

We now show that the eigenvalues of $\mathbf{A}(\mathbf{M})$ can be explicitly computed in terms of the eigenvalues of \mathbf{M} .

$\mathbf{A}(\mathbf{M})$ is a block diagonal matrix, with the final $(k-1)s$ block consisting of zeros. We therefore consider the eigenvalues of non-zero $(N-k+2)s \times (N-k+2)s$ block, which is denoted $\tilde{\mathbf{A}}(\mathbf{M})$. The entries of $\tilde{\mathbf{A}}(\mathbf{M})$ can all be written as

$$[\mathbf{A}(\mathbf{M})]_{i,j} = a_{i,j} \mathbf{M}^{r(i,j)},$$

where $a_{i,j} \in \{-1, 0, 1\}$ and $r(i,j) \in [1, 2k]$.

Suppose (μ, \mathbf{v}) is an eigenpair of \mathbf{M} . We then propose that an eigenvector of $\tilde{\mathbf{A}}(\mathbf{M})$ has the form $\mathbf{w} = [b_1 \mathbf{v}^\top, b_2 \mathbf{v}^\top, \dots, b_{N-k} \mathbf{v}^\top]^\top$ where $b_i \in \mathbb{R}$ are scalars to be computed. Hence,

$$(\tilde{\mathbf{A}}(\mathbf{M}) \mathbf{w})_i = \sum_{j=1}^{N-k} a_{i,j} b_j \mathbf{M}^{r(i,j)} \mathbf{v} = \sum_{j=1}^{N-k} a_{i,j} b_j \mu^{r(i,j)} \mathbf{v} = (\tilde{\mathbf{A}}(\mu) \mathbf{w})_i.$$

¹This is due to the reasoning $0 \leq (|a| - |b|)^2 \Leftrightarrow 2|a||b| \leq a^2 + b^2 \Leftrightarrow 4|a||b| \leq (|a| + |b|)^2$, before taking square roots and negating.

As $\tilde{\mathbf{A}}(\mu)$ is a block matrix with scalar blocks, we can eliminate \mathbf{v} and rewrite the eigenvalue equation for $\tilde{\mathbf{A}}(\mathbf{M})$ in terms of the eigenvalues of \mathbf{M} :

$$\tilde{\mathbf{A}}(\mathbf{M})\mathbf{w} = \nu\mathbf{w} \Leftrightarrow \tilde{\mathbf{A}}(\mu)\mathbf{b} = \nu\mathbf{b},$$

where $\mathbf{b} = [b_1, b_2, \dots, b_{N-k}]^\top$. We note that $\mathbf{A}(\mu) \in \mathbb{R}^{(N-k+2) \times (N-k+2)}$. For each eigenvalue μ of \mathbf{M} we can therefore find $N - k + 2$ eigenvalues of $\tilde{\mathbf{A}}(\mathbf{M})$, and their corresponding eigenvectors can be computed from the eigenvectors of $\tilde{\mathbf{A}}(\mu)$ via the definition of \mathbf{w} . \square

The result of Proposition 2 provides an inexpensive way to calculate the eigenvalues of $\mathbf{L}_M^{-\top} \mathbf{L}^\top \mathbf{L} \mathbf{L}_M^{-1}$, via the eigenvalues of a $(N - k + 2) \times (N - k + 2)$ matrix. In the following sections we consider explicit expressions for the extreme eigenvalues of $\mathbf{L}_M^{-\top} \mathbf{L}^\top \mathbf{L} \mathbf{L}_M^{-1}$ for $k = 3$ and $k = 4$, and show that incorporating model information leads to low-rank structure in $\tilde{\mathbf{A}}$ and hence many unit eigenvalues.

4.2.1 Bounds on the eigenvalues of $\mathbf{L}_M^{-\top} \mathbf{L}^\top \mathbf{L} \mathbf{L}_M^{-1}$ for $k = 3$

Using the result of Proposition 2, we provide an explicit expression for the eigenvalues of $\mathbf{L}_M^{-\top} \mathbf{L}^\top \mathbf{L} \mathbf{L}_M^{-1}$ for the case $k = 3$ for small choices of N .

Proposition 3. *For $N = 3, 4, 5$, $k = 3$, the non-unit eigenvalues ν of $\mathbf{L}_M^{-\top} \mathbf{L}^\top \mathbf{L} \mathbf{L}_M^{-1}$ are given by the explicit formula*

$$\nu = 1 + \frac{1}{2} \left(\sum_{i=1}^{N-2} \mu^{2i} \pm \sqrt{\left(\sum_{i=1}^{N-2} \mu^{2i} \right)^2 + 4 \sum_{i=1}^{N-2} \mu^{2i}} \right), \quad (12)$$

where μ denote the eigenvalues of \mathbf{M} .

Proof. For $N = 3$, $\tilde{\mathbf{A}}(\mu)$ is given by

$$\tilde{\mathbf{A}}_{N=3}(\mu) = \begin{pmatrix} \mu^2 & -\mu \\ -\mu & 0 \end{pmatrix}.$$

The characteristic polynomial is given by $\nu^2 - \nu\mu^2 - \mu^2$, which has roots given by

$$\frac{1}{2} \left(\mu^2 \pm \sqrt{\mu^4 + 4\mu^2} \right). \quad (13)$$

For $N = 4$, $\tilde{\mathbf{A}}(\mu)$ is given by

$$\tilde{\mathbf{A}}_{N=4}(\mu) = \begin{pmatrix} \mu^4 & \mu^3 & -\mu^2 \\ \mu^3 & \mu^2 & -\mu \\ -\mu^2 & -\mu & 0 \end{pmatrix}.$$

We note that this matrix is rank deficient, and hence only has two non-zero eigenvalues. The characteristic polynomial is given by $\nu^2 - \nu(\mu^2 + \mu^4) - (\mu^2 + \mu^4)$, which has roots

$$\frac{1}{2} \left(\mu^2 + \mu^4 \pm \sqrt{(\mu^2 + \mu^4)^2 + 4(\mu^2 + \mu^4)} \right). \quad (14)$$

Similarly we can show for $N = 5$ that $\tilde{\mathbf{A}}(\mu)$ also has rank 2, and its two eigenvalues are given by

$$\frac{1}{2} \left(\mu^2 + \mu^4 + \mu^6 \pm \sqrt{(\mu^2 + \mu^4 + \mu^6)^2 + 4(\mu^2 + \mu^4 + \mu^6)} \right). \quad (15)$$

Substituting (13), (14), (15) into (11), in turn, gives us the required result for $N = 3, 4, 5$. \square

Remark. *By the monotonicity of (12) the extreme eigenvalues are determined by the largest absolute value of μ . If $\mu(\mathbf{M}) \in (-1, 1)$ then the maximum eigenvalue of $\mathbf{L}_M^{-\top} \mathbf{L}^\top \mathbf{L} \mathbf{L}_M^{-1}$, for $N = 3, 4, 5$, is bounded above by*

$$\nu_{\max} = 1 + \frac{1}{2} \left(\sum_{i=1}^{N-2} 1 + \sqrt{\left(\sum_{i=1}^{N-2} 1 \right)^2 + 4 \sum_{i=1}^{N-2} 1} \right) = 1 + \frac{1}{2} \left(N - 2 + \sqrt{N^2 - 4} \right),$$

and the minimum eigenvalue of $\mathbf{L}_M^{-\top} \mathbf{L}^\top \mathbf{L} \mathbf{L}_M^{-1}$ is bounded below by

$$\nu_{\min} = 1 + \frac{1}{2} \left(\sum_{i=1}^{N-2} 1 - \sqrt{\left(\sum_{i=1}^{N-2} 1 \right)^2 + 4 \sum_{i=1}^{N-2} 1} \right) = 1 + \frac{1}{2} \left(N - 2 - \sqrt{N^2 - 4} \right).$$

If the eigenvalues of \mathbf{M} are known, the result of Proposition 2 allows us to compute the eigenvalues of $\mathbf{L}_M^{-\top} \mathbf{L}^\top \mathbf{L} \mathbf{L}_M^{-1}$ by solving $s \times (N - k + 2)$ eigenproblems. Empirically, when $\lambda(\mathbf{M}) \in [-1, 1]$ we can obtain bounds on the extreme eigenvalues using $\mu = 1$. We can also compute bounds on the maximum eigenvalue of $\mathbf{L}_M^{-\top} \mathbf{L}^\top \mathbf{L} \mathbf{L}_M^{-1}$ for any choice of N via the following proposition.

Proposition 4. *Let \mathbf{L} be defined as in (4) and \mathbf{L}_M as in Definition 1 with $\mathbf{M}_i \equiv \mathbf{M}$ for all subwindows i , where \mathbf{M} is symmetric with $-1 \leq \lambda(\mathbf{M}) \leq 1$. For $k = 3$ and $N \geq 6$,*

$$\lambda(\mathbf{L}_M^{-\top} \mathbf{L}^\top \mathbf{L} \mathbf{L}_M^{-1}) \leq \min\{N, 8\}.$$

Proof. Using Proposition 2 we may consider the eigenvalues of the matrix $\tilde{\mathbf{A}}(\mu)$ where μ are the eigenvalues of \mathbf{M} . For $N = 6$,

$$\tilde{\mathbf{A}}_{N=6}(\mu) = \begin{pmatrix} \mu^2 & -\mu & 0 & 0 & 0 \\ -\mu & \mu^6 & \mu^5 & \mu^4 & -\mu^3 \\ 0 & \mu^5 & \mu^4 & \mu^3 & -\mu^2 \\ 0 & \mu^4 & \mu^3 & \mu^2 & -\mu \\ 0 & -\mu^3 & -\mu^2 & -\mu & 0 \end{pmatrix}.$$

We now write $\tilde{\mathbf{A}}_{N=6}(\mu)$ as the sum of the following matrices, so that we may bound the eigenvalues of each term:

$$\begin{aligned} \tilde{\mathbf{A}}_{N=6}(\mu) = & \begin{pmatrix} \mu^2 & 0 & 0 & 0 & 0 \\ 0 & 0 & \mu^5 & 0 & 0 \\ 0 & \mu^5 & 0 & 0 & 0 \\ 0 & 0 & 0 & 0 & -\mu \\ 0 & 0 & 0 & -\mu & 0 \end{pmatrix} + \begin{pmatrix} 0 & -\mu & 0 & 0 & 0 \\ -\mu & 0 & 0 & 0 & 0 \\ 0 & 0 & 0 & 0 & -\mu^2 \\ 0 & 0 & 0 & \mu^2 & 0 \\ 0 & 0 & -\mu^2 & 0 & 0 \end{pmatrix} + \mu^3 \begin{pmatrix} 0 & 0 & 0 & 0 & 0 \\ 0 & 0 & 0 & 0 & -1 \\ 0 & 0 & 0 & 1 & 0 \\ 0 & 0 & 1 & 0 & 0 \\ 0 & -1 & 0 & 0 & 0 \end{pmatrix} \\ & + \mu^4 \begin{pmatrix} 0 & 0 & 0 & 0 & 0 \\ 0 & 0 & 0 & 1 & 0 \\ 0 & 0 & 1 & 0 & 0 \\ 0 & 1 & 0 & 0 & 0 \\ 0 & 0 & 0 & 0 & 0 \end{pmatrix} + \mu^6 \begin{pmatrix} 0 & 0 & 0 & 0 & 0 \\ 0 & 1 & 0 & 0 & 0 \\ 0 & 0 & 0 & 0 & 0 \\ 0 & 0 & 0 & 0 & 0 \\ 0 & 0 & 0 & 0 & 0 \end{pmatrix}. \end{aligned}$$

As all matrices considered are symmetric, by [4, Fact 5.12.2] we can bound the eigenvalues of $\tilde{\mathbf{A}}_{N=6}(\mu)$ above by

$$\lambda(\tilde{\mathbf{A}}_{N=6}(\mu)) \leq \max\{\mu^2, \pm\mu^5, \pm\mu\} + \max\{\pm\mu, \mu^2\} + |\mu^3| + \mu^4 + \mu^6.$$

We see that this bound is maximised when using the largest eigenvalue of \mathbf{M} . As $|\mu| \leq 1$ by assumption

$$\max\{\lambda(\tilde{\mathbf{A}}_{N=6})\} \leq 2|\mu_{\max}| + |\mu_{\max}^3| + \mu_{\max}^4 + \mu_{\max}^6 \leq 5,$$

where μ_{\max} is the eigenvalue of largest magnitude of \mathbf{M} . Therefore the eigenvalues of $\mathbf{L}_M^{-\top} \mathbf{L}^\top \mathbf{L} \mathbf{L}_M^{-1}$ are bounded above by $1 + \max\{\lambda(\tilde{\mathbf{A}}_{N=6})\} = 6$, as required.

For other choices of N we can use a similar approach to split up $\tilde{\mathbf{A}}(\mu)$ into the sum of block diagonal matrices. We note that the number of block matrices required is controlled by the $(k - 1)$ th row/column which has $N - 1$ distinct entries. Hence for $N = 7$ and $N = 8$ we obtain the desired upper bounds on the eigenvalues of $\mathbf{L}_M^{-\top} \mathbf{L}^\top \mathbf{L} \mathbf{L}_M^{-1}$.

For $N > 8$ we apply the same argument as for the case $N = 8$: group together each power of μ in its own matrix, and split alternating anti-diagonals of μ^3 terms into two matrices. This means that for any value of N larger than 8 we can write $\tilde{\mathbf{A}}(\mu)$ as the sum of 7 block diagonal matrices, each of which has eigenvalues bounded above by 1. Therefore for $N \geq 8$ the eigenvalues of $\mathbf{L}_M^{-\top} \mathbf{L}^\top \mathbf{L} \mathbf{L}_M^{-1}$ are bounded above by 8 as required. \square

Remark. A similar approach is not illustrative when examining a lower bound for the eigenvalues, as this would yield negative bounds, whereas all eigenvalues of $\mathbf{L}_M^{-\top} \mathbf{L}^\top \mathbf{L} \mathbf{L}_M^{-1}$ are clearly greater than zero by construction.

Proposition 5. Let \mathbf{L} be defined as in (4) and \mathbf{L}_M as in Definition 1 with $\mathbf{M}_i \equiv \mathbf{M}$ for N subwindows i , where $\mathbf{M} \in \mathbb{R}^{s \times s}$ is symmetric with $-1 \leq \lambda(\mathbf{M}) \leq 1$. For $k = 3$ and $N \geq 3$, $\mathbf{L}_M^{-\top} \mathbf{L}^\top \mathbf{L} \mathbf{L}_M^{-1}$ has $(2+i)s$ unit eigenvalues, where

$$i = \left\lfloor \frac{N-3}{3} \right\rfloor + N - 3 \left\lfloor \frac{N}{3} \right\rfloor.$$

Proof. We show this by constructing the eigenvectors of $\mathbf{L}_M^{-\top} \mathbf{L}^\top \mathbf{L} \mathbf{L}_M^{-1}$ corresponding to a zero eigenvalue, noting that eigenvectors of $\mathbf{A}(\mathbf{M})$ corresponding to zero eigenvalues are eigenvectors of $\mathbf{L}_M^{-\top} \mathbf{L}^\top \mathbf{L} \mathbf{L}_M^{-1}$ for unit eigenvalues.

For $k = 3$ and all choices of N , we obtain $2s$ unit eigenvalues from the final $(k-1)s \times (k-1)s$ identity block. We now consider

$$\tilde{\mathbf{A}}_{N=4}(\mu) = \begin{pmatrix} \mu^4 & \mu^3 & -\mu^2 \\ \mu^3 & \mu^2 & -\mu \\ -\mu^2 & -\mu & 0 \end{pmatrix}, \quad (16)$$

which has rank 2, and an eigenvector given by $[1, -\mu, 0]^\top$ corresponding to a zero eigenvalue. This means that we can construct s linearly independent eigenvectors corresponding to zero eigenvalues of $\tilde{\mathbf{A}}_{N=4}(\mathbf{M})$ via $\mathbf{w} = [\mathbf{v}_i^\top, -\mu_i \mathbf{v}_i^\top, \mathbf{0}^\top]^\top$, where (μ_i, \mathbf{v}_i) are eigenpairs of \mathbf{M} .

For more general $\tilde{\mathbf{A}}(\mathbf{M})$, we start at the end of the matrix and move backward towards the first block. For each $(k+1)s \times (k+1)s$ block, excluding the first, we use a similar idea to construct s linearly independent eigenvectors corresponding to zero eigenvalues. These take the form $[\mathbf{0}^\top, \mathbf{0}^\top, \dots, \mathbf{0}^\top, -\mathbf{v}_i^\top, \mu_i \mathbf{v}_i^\top, \mathbf{0}^\top, \mathbf{0}^\top, \dots, \mathbf{0}^\top]^\top$, where the non-zero terms align with the middle of the blocks of $\tilde{\mathbf{A}}(\mathbf{M})$. The number of these blocks is determined by $\lfloor (N-3)/3 \rfloor$.

The first block can yield additional zero eigenvalues of $\tilde{\mathbf{A}}(\mathbf{M})$. If the first block is given by (16), we obtain s zero eigenvalues following the same argument as above. If the first block is ‘complete’, i.e. given by

$$\tilde{\mathbf{A}}_{N=5}(\mu) = \begin{pmatrix} \mu^6 & \mu^5 & \mu^4 & -\mu^3 \\ \mu^5 & \mu^4 & \mu^3 & -\mu^2 \\ \mu^4 & \mu^3 & \mu^2 & -\mu \\ -\mu^3 & -\mu^2 & -\mu & 0 \end{pmatrix},$$

this has rank 2, with eigenvectors that correspond to zero eigenvalues given by $[1, -2\mu, \mu^2, 0]^\top$ and $[1, \mu^2, -2\mu^2, 0]^\top$. Hence, we can find $2s$ linearly independent eigenvectors for 0 via $[\mathbf{v}_i^\top, \mu_i^2 \mathbf{v}_i^\top, -2\mu_i^2 \mathbf{v}_i^\top, \mathbf{0}^\top, \mathbf{0}^\top, \dots, \mathbf{0}^\top]^\top$ and $[\mathbf{v}_i^\top, -2\mu_i^2 \mathbf{v}_i^\top, \mu_i^2 \mathbf{v}_i^\top, \mathbf{0}^\top, \mathbf{0}^\top, \dots, \mathbf{0}^\top]^\top$. The number of independent eigenvectors contributed by this first block is therefore given by ρs , where $\rho = N - 3 \lfloor \frac{N}{3} \rfloor$.

Hence the total number of unit eigenvalues is given by $(2+i)s$, with i defined in the proposition statement. \square

4.2.2 Eigenvalues of $\mathbf{L}_M^{-\top} \mathbf{L}^\top \mathbf{L} \mathbf{L}_M^{-1}$ for $k = 4$

We may use similar arguments to obtain bounds for the case $k = 4$. However, such bounds are much more pessimistic in this case, so we employ another approach that allows us to achieve stronger results.

Proposition 6. Let \mathbf{L} be defined as in (4) and \mathbf{L}_M as in Definition 1 with $\mathbf{M}_i \equiv \mathbf{M}$ for all subwindows i , where \mathbf{M} is symmetric with $-1 \leq \lambda(\mathbf{M}) \leq 1$. For $k = 4$ and $N \geq 4$,

$$\lambda(\mathbf{L}_M^{-\top} \mathbf{L}^\top \mathbf{L} \mathbf{L}_M^{-1}) \leq \min\{N-1, 10\}.$$

Proof. This is proved by following the same approach as in Proposition 4. \square

Remark. This argument can be extended to any value of k and the upper bound is given by $2k+2$ (this is the maximum number of terms in a row/column plus one for the single duplicated term). However, we expect this bound to be pessimistic.

By using a different splitting to Proposition 6 we can improve on the bound for some choices of N .

Proposition 7. Let \mathbf{L} be defined as in (4) and \mathbf{L}_M as in Definition 1 with $\mathbf{M}_i \equiv \mathbf{M}$ for all subwindows i , where \mathbf{M} is symmetric with $-1 \leq \lambda(\mathbf{M}) \leq 1$. For $k = 4$ and $N = 9, 10$,

$$\lambda(\mathbf{L}_M^{-\top} \mathbf{L}^\top \mathbf{L} \mathbf{L}_M^{-1}) \leq \frac{5 + \sqrt{21}}{2} + \sqrt{N - 3}.$$

Proof. We split $\mathbf{A}_{N=9}(\mu)$ into two matrices:

$$\mathbf{A}_{N=9}(\lambda) = \begin{pmatrix} \mu^4 & \mu^3 & 0 & 0 & 0 & 0 & 0 \\ \mu^3 & \mu^2 & 0 & 0 & 0 & 0 & 0 \\ 0 & 0 & \mu^8 & 0 & 0 & 0 & 0 \\ 0 & 0 & 0 & \mu^6 & \mu^5 & \mu^4 & -\mu^3 \\ 0 & 0 & 0 & \mu^5 & \mu^4 & \mu^3 & -\mu^2 \\ 0 & 0 & 0 & \mu^4 & \mu^3 & \mu^2 & -\mu \\ 0 & 0 & 0 & -\mu^3 & -\mu^2 & -\mu & 0 \end{pmatrix} + \begin{pmatrix} 0 & 0 & -\mu^2 & 0 & 0 & 0 & 0 \\ 0 & 0 & -\mu & 0 & 0 & 0 & 0 \\ -\mu^2 & -\mu & 0 & \mu^7 & \mu^6 & \mu^5 & -\mu^5 \\ 0 & 0 & \mu^7 & 0 & 0 & 0 & 0 \\ 0 & 0 & \mu^6 & 0 & 0 & 0 & 0 \\ 0 & 0 & \mu^5 & 0 & 0 & 0 & 0 \\ 0 & 0 & -\mu^4 & 0 & 0 & 0 & 0 \end{pmatrix}.$$

The maximum eigenvalue of the first term is maximised when $\mu = 1$:

$$\max \left\{ \frac{1}{2}(3 + \sqrt{21}), 1, 2 \right\} = \frac{3 + \sqrt{21}}{2}.$$

The second matrix has rank 2, and the non-zero eigenvalues are given by

$$\nu = \pm \sqrt{\mu^2 + \mu^4 + \mu^8 + \mu^{10} + \mu^{12} + \mu^{14}}.$$

This expression is maximised by the largest eigenvalue of \mathbf{M} , which is bounded above by 1. Therefore $\nu \leq \sqrt{6}$, and the new upper bound is given by $\frac{5 + \sqrt{21}}{2} + \sqrt{6}$ is required.

Following a similar strategy, for $N = 10$ the upper bound on the first term is the same as $\max\{\frac{1}{2}(3 + \sqrt{21}), 1, 3\} = \frac{1}{2}(3 + \sqrt{21})$. The second matrix has an extra term of $-\mu^3$ in the fifth row/column. This means that the expression for the upper bound is given by

$$\nu = \pm \sqrt{\mu^2 + \mu^4 + \mu^6 + \mu^8 + \mu^{10} + \mu^{12} + \mu^{14}} \leq 7.$$

□

Remark. For $N = 11$ the final block in the first matrix has maximum eigenvalue 4, meaning that the bound is given by $5 + \sqrt{8}$.

Remark. A similar approach can be used for the $k = 3$ case, but it is only beneficial for $N = 9$ where the new bound is given by $4 + \sqrt{6} < 7.5$. For larger choices of N the bound given with this approach exceeds the existing value of 8 obtained in Proposition 4.

Remark. For larger N by a good choice of splitting we can improve slightly on the existing bound of 10. For alternate blocks, we have blocks of $9s$ ‘cross’ matrices, and the remaining terms $(3s - 4s)$ which are block diagonal and can have their eigenvalues bounded in the same way as in Proposition 7 by $\sqrt{4} = 2$. This splitting works for any choice of N and results in an upper bound of $7 + \sqrt{8} < 10$. One can improve on this bound slightly if the last block is ‘incomplete’, in which case the bound is given by $5 + \sqrt{8} + \sqrt{3}$.

We can also derive similar result to Proposition 5, where $3s$ units come from the trailing identity block, each subsequent $5s$ block adds $2s$ unit eigenvalues, and the final block can add $(1 - 3)s$ units depending on its size.

Proposition 8. Let \mathbf{L} be defined as in (4) with $\mathbf{M}_i \equiv \mathbf{M}$ for N subwindows i , where $\mathbf{M} \in \mathbb{R}^{s \times s}$ is symmetric with $-1 \leq \lambda(\mathbf{M}) \leq 1$. For $k = 4$ and $N \geq 4$, $\mathbf{L}_M^{-\top} \mathbf{L}^\top \mathbf{L} \mathbf{L}_M^{-1}$ has $(3 + i)s$ unit eigenvalues where

$$i = 2 \left\lfloor \frac{N - 5}{4} \right\rfloor + N - 4 \left\lfloor \frac{N}{4} \right\rfloor.$$

Proof. This is proved by following the same approach as in Proposition 5. □

Remark. *It is possible to derive similar results for larger values of k , with analysis of increasing complexity as k increases. The results of this section correspond to the most pessimistic case of dropping many terms in \mathbf{L}_M and \mathbf{L}_M^\top within the preconditioner, and indicate that dropping fewer terms (corresponding to larger k) would continue to yield an accurate preconditioner.*

This analysis shows that as we increase k we increase the number of unit eigenvalues that are ‘recovered’ by the preconditioned system. We can determine the minimum eigenvalues of $\mathbf{L}_M^{-\top} \mathbf{L}^\top \mathbf{L} \mathbf{L}_M^{-1}$ directly by computing the smallest eigenvalues of $\tilde{\mathbf{A}}(\mu)$. As $\mathbf{L}_M^{-\top} \mathbf{L}^\top \mathbf{L} \mathbf{L}_M^{-1}$ is positive definite its smallest eigenvalues are bounded below by zero for any choice of k . Improved bounds on the smallest eigenvalues cannot be obtained using the splitting approach of Proposition 6 which yields negative lower bounds in this setting. We believe that $k = 3$ and $k = 4$ are likely to provide a good balance between computational efficiency per iteration and reduced number of iterations within a MINRES/GMRES routine, and as a rule of thumb increasing k (that is, dropping fewer terms in \mathbf{L}) should typically improve the rate of convergence.

5 Approximations of $\hat{\mathbf{R}}$

Theorem 1 suggests that the eigenvalues of the preconditioned system are also influenced by the quality of the approximation of $\hat{\mathbf{R}}$ to \mathbf{R} in the preconditioner. In this section we consider four choices of $\hat{\mathbf{R}}$. Similarly to the preconditioners for \mathbf{L} , we consider an existing choice of preconditioner that is diagonal, and three new choices of preconditioner that include correlation information. We expect the new preconditioners to be beneficial for highly correlated \mathbf{R} matrices.

5.1 Parallelisable choices of $\hat{\mathbf{R}}$

Many previous studies of the saddle point data assimilation formulation assume that \mathbf{R} is diagonal or easy to invert [15, 12]. However for more complicated structures, it is unlikely that using the exact inverse of \mathbf{R} would be efficient in terms of storage or computation.

The first two choices of $\hat{\mathbf{R}}$ considered in this section allow for additional parallelisation of the saddle point implementation. The first preconditioner, \mathbf{R}_{diag} defined in Algorithm 1, takes the diagonal of the original observation error covariance matrix \mathbf{R} . This is often a first approximation of \mathbf{R} or its inverse for simple covariance structures. This choice of $\hat{\mathbf{R}}$ is cheap to apply and highly parallelisable, but is expected to perform poorly if there is significant off-diagonal correlation structure.

Algorithm 1: Diagonal preconditioner method
$1 \text{ Set } \mathbf{R}_{diag}(i, j) = \begin{cases} \mathbf{R}(i, i) & \text{if } i = j, \\ 0 & \text{if } i \neq j. \end{cases}$

The second parallelisable choice of $\hat{\mathbf{R}}$, \mathbf{R}_{block} in Algorithm 2, is designed to exploit existing block structure in \mathbf{R} . In applications, \mathbf{R} itself often has a block structure, with the strength of off-diagonal correlations varying, e.g. for different instruments or measurement types. The idea of \mathbf{R}_{block} is to retain the sub/super-diagonal blocks of \mathbf{R} with the largest norm. Neglecting off-diagonal blocks of \mathbf{R} with smaller norm ensures that \mathbf{R}_{block} is decoupled into a block diagonal matrix, which can then be applied in parallel. Algorithm 2 allows users to control the size of each block and the number of processors being used.

We note that if two adjacent blocks are retained, then we retain $\mathbf{R}(\text{pvec}(1) : \text{pvec}(3), \text{pvec}(1) : \text{pvec}(3))$, i.e. the second block sub- and super-diagonals are included even though we have not measured their norm. This does not lead to a large increase the cost of inversion, as the overall matrix block structure is unchanged, and we deem that retaining the additional correlation information is likely to be beneficial for the preconditioner.

5.2 Preconditioning methods motivated by reconditioning

The next two choices of $\hat{\mathbf{R}}$ are motivated by reconditioning methods [36]. These are commonly used in data assimilation implementations to mitigate the issues associated with ill-conditioned sample covariance matrices [40]. In this application we consider the use of such methods to develop new terms in the preconditioner only.

Algorithm 2: Block preconditioner method

```

1 Inputs:  $\mathbf{R}$ ,  $\mathbf{pvec}$  = vector of block sizes,  $\mathbf{tol}$  = tolerance for retaining blocks,  $\mathbf{maxsize}$  = maximum size
  permitted on a single processor,  $\mathbf{numproc}$  = number of available processors.
2 Compute  $\mathbf{p} = \mathbf{sum}(\mathbf{pvec})$ ,  $\mathbf{pn} = |\mathbf{pvec}|$ .
3 Define  $\mathbf{pst}$  = starting index for each new block.
4 Initialise  $\mathbf{R}_{block} = \mathbf{R}$ .
5 for  $i = 1:\mathbf{pn}-1$ 
6   Compute scaled Frobenius norm of super-diagonal blocks via  $\mathbf{normvec}(i) = \dots$ 
7    $\mathbf{norm}(\mathbf{R}(\mathbf{pst}(i):\mathbf{pst}(i+1)-1, \mathbf{pst}(i+1):\mathbf{pst}(i+2)-1), 'fro')/\mathbf{sqrt}(\mathbf{pvec}(i)*\mathbf{pvec}(i+1))$ .
8 end
9 Retain blocks where  $\mathbf{normvec}(i) > \mathbf{tol}$ :
10 for  $i = 1:\mathbf{pn}-1$ 
11   if  $\mathbf{normvec}(i) < \mathbf{tol}$ 
12     Set  $\mathbf{R}_{block}(\mathbf{pst}(i+1):\mathbf{p}, 1:\mathbf{pst}(i+1)-1) = 0$ 
13     Set  $\mathbf{R}_{block}(1:\mathbf{pst}(i+1)-1, \mathbf{pst}(i+1):\mathbf{p}) = 0$ 
14   end
15 end
16 if size of largest block  $> \mathbf{maxsize}$ 
17   split largest block into two components.
18 end
19 if number of distinct blocks  $> \mathbf{numproc}$ 
20   combine two smallest adjacent blocks in  $\mathbf{R}_{block}$ .
21 elseif number of distinct blocks  $< \mathbf{numproc} - 2$ 
22   split largest block of  $\mathbf{R}_{block}$  into two components.
23 end

```

Algorithm 3: Ridge regression method

```

1 Inputs: Matrix  $\mathbf{R}$ , target condition number  $\kappa_{\max}$ . Define  $\gamma = \frac{\lambda_{\max}(\mathbf{R}) - \lambda_{\min}(\mathbf{R})\kappa_{\max}}{\kappa_{\max} - 1}$ .
2 Set  $\mathbf{R}_{RR} = \mathbf{R} + \gamma\mathbf{I}$ .

```

Algorithms 3 and 4 define parameter-dependent preconditioners. Typically in the reconditioning setting γ and T are selected such that reconditioned matrices have condition number κ_{\max} . However, in the preconditioning approach we select γ and T directly, with larger parameter values yielding smaller condition numbers of $\widehat{\mathbf{R}}$.

Algorithms 3 and 4 can be used to construct preconditioners for \mathbf{R} that retain much of the structure of the original matrix, but are better conditioned. Additionally we can prove how the eigenvalues of the preconditioned term that appears in Theorem 1 change as we vary γ and T respectively. The following lemmas determine the spectra of the preconditioned terms $\mathbf{R}_{RR}^{-1}\mathbf{R}$ and $\mathbf{R}_{ME}^{-1}\mathbf{R}$ for any choice of parameters γ and T .

Lemma 2. *The eigenvalues of $\mathbf{R}_{RR}^{-1}\mathbf{R}$ are given by*

$$\lambda(\mathbf{R}_{RR}^{-1}\mathbf{R}) = \frac{\lambda_i(\mathbf{R})}{\lambda_i(\mathbf{R}) + \gamma},$$

where $\lambda_i(\mathbf{R})$ denote the eigenvalues of \mathbf{R} .

Proof. Let $\mathbf{R} = \mathbf{V}\mathbf{\Lambda}\mathbf{V}^\top$, where $\mathbf{\Lambda} = \mathbf{diag}(\lambda_i)$, be the eigendecomposition of \mathbf{R} . Then

$$\mathbf{R}_{RR} = \mathbf{V}(\mathbf{\Lambda} + \gamma\mathbf{I})\mathbf{V}^\top$$

and hence

$$\mathbf{R}_{RR}^{-1}\mathbf{R} = \mathbf{V} \left(\mathbf{diag} \left(\frac{\lambda_i}{\lambda_i + \gamma} \right) \right) \mathbf{V}^\top.$$

□

Algorithm 4: Minimum eigenvalue method

- 1 Inputs: Matrix $\mathbf{R} = \mathbf{V}\mathbf{\Lambda}\mathbf{V}^\top$, target condition number κ_{\max} . Set $\lambda_{\max}(\mathbf{R}_{ME}) = \lambda_{\max}(\mathbf{R})$.
- 2 Define $T = \frac{\lambda_{\max}(\mathbf{R})}{\kappa_{\max}} > \lambda_{\min}(\mathbf{R})$.
- 3 Set the remaining eigenvalues of \mathbf{R}_{ME} via

$$\lambda_k(\mathbf{R}_{ME}) = \begin{cases} \lambda_k(\mathbf{R}) & \text{if } \lambda_k(\mathbf{R}) > T, \\ T & \text{if } \lambda_k(\mathbf{R}) \leq T. \end{cases}$$

- 4 Construct the reconditioned matrix via $\mathbf{R}_{ME} = \mathbf{V}\mathbf{\Lambda}_{ME}\mathbf{V}^\top$, where $\mathbf{\Lambda}_{ME}(i, i) = \lambda_i(\mathbf{R}_{ME})$.

We note that for any value of γ , $0 < \lambda(\mathbf{R}_{RR}^{-1}\mathbf{R}) < 1$. For small values of γ all eigenvalues are closer to 1 and as γ increases, more eigenvalues move towards zero.

Lemma 3. *The eigenvalues of $\mathbf{R}_{ME}^{-1}\mathbf{R}$ are given by*

$$\lambda_i(\mathbf{R}_{ME}^{-1}\mathbf{R}) = \begin{cases} 1 & \text{if } \lambda_i > T, \\ \frac{\lambda_i}{T} < 1 & \text{if } \lambda_i \leq T. \end{cases}$$

Proof. Let $\mathbf{R} = \mathbf{V}\mathbf{\Lambda}\mathbf{V}^\top$, where $\mathbf{\Lambda} = \text{diag}(\lambda_i)$, be the eigendecomposition of \mathbf{R} . Then

$$\mathbf{R}_{ME} = \mathbf{V}\mathbf{\Lambda}_{ME}\mathbf{V}^\top,$$

where $\mathbf{\Lambda}_{ME}(i, i) = \max\{T, \lambda_i(\mathbf{R})\}$. Hence

$$\mathbf{R}_{ME}^{-1}\mathbf{R} = \mathbf{V} \left(\text{diag} \left(\frac{\lambda_i}{\max\{T, \lambda_i\}} \right) \right) \mathbf{V}^\top,$$

which has eigenvalues corresponding to the expression in the theorem statement. \square

Again all of the eigenvalues of $\mathbf{R}_{ME}^{-1}\mathbf{R}$ lie in the range $(0,1]$. For small values of T most of the eigenvalues are units, with a few smaller than 1. As T increases a larger number of eigenvalues become strictly smaller than 1.

Therefore both choices of preconditioner maintain the ordering of eigenvalues and yield preconditioned spectra lying between 0 and 1. For both approaches increasing the parameter leads to larger differences between the preconditioned spectra and 1. However, smaller parameter values may yield choices of $\hat{\mathbf{R}}$ that are ill-conditioned, and hence expensive to evaluate as part of a preconditioner. A natural question is therefore how to select appropriate parameter values, and how this can be implemented automatically. Heuristics for automated parameter selection are discussed in the following section for specific numerical experiments, but it is likely that some initial investigation would be necessary to identify suitable methods for specific problems of interest.

In Section 7 we compare the performance of the four approximations \mathbf{R}_{diag} , \mathbf{R}_{block} , \mathbf{R}_{RR} , and \mathbf{R}_{ME} .

6 Numerical framework

In this section we introduce the numerical framework for the experiments presented in Section 7. We begin by introducing two problems of interest: a linear partial differential equation in Section 6.1 and a system of non-linear coupled ordinary differential equations in Section 6.2. We present the discretised models \mathbf{M}_i and discuss how the properties of \mathbf{M}_i relate to the assumptions required for the theory introduced in Section 4. In Section 6.3 we then define the parameters for the data assimilation problem. The same data assimilation framework is used for both problems. We note that all results are computed using MATLAB version 2019b.

6.1 Heat equation with Dirichlet boundary conditions

The first problem of interest is the one-dimensional heat equation on the unit line

$$\frac{\partial u}{\partial t} = \alpha \frac{\partial^2 u}{\partial x^2}, \quad (17)$$

with Dirichlet boundary conditions $u(0, t) = u_0, u(1, t) = u_1 \forall t$. We discretise (17) using the forward Euler method in time and second-order centred differences in space. This means we can write the model evolution in matrix form for a single time model step as $\mathbf{u}^{t+\Delta t} = \mathbf{M}_{\Delta t} \mathbf{u}^t$, where $\mathbf{M}_{\Delta t}$ denotes the application of a single model time-step of length Δt to the heat equation with Dirichlet boundary conditions; this is given by

$$\mathbf{M}_{\Delta t} = \begin{pmatrix} 0 & 0 & 0 & 0 & \cdots & 0 \\ 0 & 1-2r & r & 0 & \cdots & 0 \\ 0 & r & 1-2r & \ddots & & \vdots \\ 0 & 0 & \ddots & \ddots & r & 0 \\ \vdots & \vdots & & & r & 1-2r & 0 \\ 0 & 0 & \cdots & 0 & 0 & 0 & 0 \end{pmatrix}, \quad (18)$$

where $r = \frac{\alpha \Delta t}{(\Delta x)^2}$. Noting that the eigenvalues of (18) have absolute value strictly less than 1, we may apply the theory in Section 4.1.

Lemma 4. *If $r \leq \frac{1}{2}$, the eigenvalues of $\mathbf{M}_{\Delta t}$ lie in the range $(-1, 1)$.*

Proof. We obtain two zero eigenvalues of $\mathbf{M}_{\Delta t}$ from the Dirichlet boundary conditions. As the central block is tridiagonal we can compute the remaining eigenvalues immediately via the formula:

$$\lambda(\mathbf{M}_{\Delta t}) = 1 - 2r - 2r \cos\left(\frac{k\pi}{s-1}\right) = 1 - 2r \left(1 + \cos\left(\frac{k\pi}{s-1}\right)\right), \quad k = 1, \dots, s-2.$$

Letting $r \leq \frac{1}{2}$, which is required for the numerical method to be stable, the result follows. \square

Therefore (18) satisfies the assumptions on the results in Section 4.1, and we can determine the extreme eigenvalues of $\widehat{\mathbf{L}}^{-\top} \mathbf{L}^\top \mathbf{L} \widehat{\mathbf{L}}^{-1}$ by considering the eigenvalues of $\mathbf{M}_{\Delta t}$. We may now compute the bounds on the eigenvalues of $\mathbf{L}^\top \mathbf{L}$. We note first that although the evolution between two model time-steps is given by $\mathbf{M}_{\Delta t}$, in the data assimilation problem we use \mathbf{M} to denote the linear model between observation times. This is given by $\mathbf{M}_{\Delta t}$ raised to the appropriate power. Due to Lemma 4 the eigenvalues of \mathbf{M} are also bounded as $-1 < \lambda(\mathbf{M}) < 1$. In particular if an even number of model time-steps is used then \mathbf{M} is positive semi-definite and the eigenvalues of \mathbf{M} lie in the range $0 \leq \lambda(\mathbf{M}) < 1$. Therefore all the theoretical assumptions of Section 4 are satisfied.

Corollary 1. *If \mathbf{M} represents the heat equation with Dirichlet boundary conditions, the eigenvalues of $\mathbf{L}^\top \mathbf{L}$ satisfy*

$$0 < \lambda(\mathbf{L}^\top \mathbf{L}) < 4.$$

Proof. The lower bound immediately follows due to the structure of $\mathbf{L}^\top \mathbf{L}$ and the fact it is invertible. Using the bound given by Proposition 1, with the bounds on the eigenvalues of \mathbf{M} given by Lemma 4, we obtain

$$\lambda(\mathbf{L}^\top \mathbf{L}) < 1 + 1^2 + 2 \times 1 = 4.$$

\square

For the numerical experiments presented in Section 7 we fix $\alpha = 1$ and vary spatial and temporal resolutions together. Specifically, we set the ratio $r = \frac{\Delta t}{(\Delta x)^2} = 0.4$ for all experiments.

We now consider the bounds on the eigenvalues of $\mathbf{L}^\top \mathbf{L}$ and $\mathbf{L}_M^{-\top} \mathbf{L}^\top \mathbf{L} \mathbf{L}_M^{-1}$ that were developed in Section 4.1 for \mathbf{M} defined above. Table 1 shows how the extreme eigenvalues of $\mathbf{L}^\top \mathbf{L}$ change with increasing subwindows N for a fixed time-discretisation. The lower and upper bounds given by Propositions 1 and 2 are independent of the number of sub-windows, and hence these do not change with increasing N . We consider $\mathbf{M} = \mathbf{M}_{\Delta t}^2$ so that the assumption of positive definiteness for Proposition 2 is satisfied. For $\mathbf{M} = \mathbf{M}_{\Delta t}^2$ the largest eigenvalue of \mathbf{M} is so close to one that the lower bound is effectively 0. Table 1 shows that as N increases the largest eigenvalue of $\mathbf{L}^\top \mathbf{L}$

Table 1: Eigenvalues of $\mathbf{L}^\top \mathbf{L}$ for $\mathbf{M} = \mathbf{M}_{\Delta t}^2$ and $s = 500$, for different numbers of observation subwindows: lower bound computed using Proposition 2, minimum/maximum eigenvalues computed using the `eigs` function in MATLAB, upper bound given by Proposition 1.

$N + 1$	Lower bound	Minimum eigenvalue	Maximum eigenvalue	Upper bound
3	8.3323×10^{-30}	0.1981	3.2470	4
4	8.3323×10^{-30}	0.1206	3.5321	4
5	8.3323×10^{-30}	0.0810	3.6825	4
6	8.3323×10^{-30}	0.0581	3.7709	4
7	8.3323×10^{-30}	0.0437	3.8271	4
8	8.3323×10^{-30}	0.0341	3.8649	4
9	8.3323×10^{-30}	0.0273	3.8916	4
10	8.3323×10^{-30}	0.0223	3.9111	4
11	8.3323×10^{-30}	0.0186	3.9258	4
12	8.3323×10^{-30}	0.0158	3.9372	4
13	8.3323×10^{-30}	0.0135	3.9461	4

Table 2: Eigenvalues of $\mathbf{L}_M^{-\top} \mathbf{L}^\top \mathbf{L} \mathbf{L}_M^{-1}$ for $s = 500$ and $k = 3$ (skipping every third block), for different numbers of observation subwindows: number of unit eigenvalues given by Proposition 5, minimum/maximum eigenvalues computed using the `eigs` function in MATLAB, upper bound given by Proposition 4.

$N + 1$	No. unit eigenvalues	Minimum eigenvalue	Maximum eigenvalue	Upper bound
4	1000	0.3820	2.6180	3
5	1500	0.2679	3.7321	4
6	2000	0.2087	4.7913	5
7	1500	0.1514	4.8931	6
8	2000	0.1170	5.1052	7
9	2500	0.0950	5.5549	7.5
10	2000	0.0764	5.5943	8
11	2500	0.0632	5.6748	8
12	3000	0.0536	5.8802	8
13	2500	0.0454	5.8989	8

Table 3: Eigenvalues of $\mathbf{L}_M^{-\top} \mathbf{L}^\top \mathbf{L} \mathbf{L}_M^{-1}$ for $s = 500$ and $k = 4$ (skipping every fourth block), for different numbers of observation subwindows: number of unit eigenvalues given by Proposition 8, minimum/maximum eigenvalues computed using the `eigs` function in MATLAB, upper bound given by Propositions 6 and 7.

$N + 1$	No. unit eigenvalues	Minimum eigenvalue	Maximum eigenvalue	Upper bound
4	1600	1	1	1
5	1600	0.3820	2.6180	3
6	2000	0.2679	3.7321	4
7	2400	0.2087	4.7913	5
8	2000	0.1716	5.8284	6
9	2400	0.1336	5.8857	7
10	2800	0.1072	5.9880	7.2408
11	3200	0.0890	6.1955	7.4370
12	2800	0.0758	6.6260	7.8284
13	3200	0.0641	6.6491	10

quickly approaches the upper bound. The smallest eigenvalue decreases with increasing N , but is bounded further away from 0 than is indicated by the lower bound.

Tables 2 and 3 show the number of unit eigenvalues and the upper bound on the eigenvalues given by Propositions 4, 6, 7 as N is increased for $k = 3$ and $k = 4$ respectively. For the same choice of N and with both values of k , preconditioning with \mathbf{L}_M increases the smallest eigenvalue of the product compared to using no preconditioner. The smallest eigenvalue is larger for $k = 4$ than $k = 3$ for all choices of N . Increasing N decreases the minimum eigenvalue of $\mathbf{L}_M^\top \mathbf{L}^\top \mathbf{L} \mathbf{L}_M^{-1}$ and increases the largest eigenvalue for both choices of k . For small values of N , the largest eigenvalue of the product is smaller when using \mathbf{L}_M than when using \mathbf{L}_0 . For $N > 6$ (respectively $N > 7$) the largest eigenvalue using \mathbf{L}_M with $k = 3$ (respectively $k = 4$) exceeds 4 which is the upper bound for eigenvalues of $\mathbf{L}^\top \mathbf{L}$. The upper bound is not tight for either value of k .

Therefore, for all choices of $\hat{\mathbf{L}}$, increasing the number of subwindows leads to smaller minimum eigenvalues and larger maximum eigenvalues. Using \mathbf{L}_M leads to larger maximum eigenvalues, but there are many more unit eigenvalues of the preconditioned system than arise when preconditioning with \mathbf{L}_0 . For the heat equation, changing the discretisation (i.e. increasing s) has negligible effect on the extreme eigenvalues of $\mathbf{L}^\top \mathbf{L}$ and $\mathbf{L}_M^{-\top} \mathbf{L}^\top \mathbf{L} \mathbf{L}_M^{-1}$.

As the saddle point matrix for the heat equation, \mathcal{A} , is symmetric, we can apply MINRES with the block diagonal preconditioner, and apply the theory of Sections 3 and 4 directly. In Section 7.2 we also consider the inexact constraint preconditioner with GMRES, as this has been found to perform well for the data assimilation saddle point problem numerically [13, 15].

6.2 Lorenz 96 model

The second problem of interest concerns the Lorenz 96 model [24], a non-linear problem that is often considered as a test problem for data assimilation applications (see for example [8, 18] for use within the saddle point formulation for data assimilation). The Lorenz 96 model consists of s coupled ordinary differential equations which are discrete in space and continuous in time. Consider s equally spaced points on the unit line, i.e. $\Delta x = \frac{1}{s}$. For $i = 1, \dots, s$,

$$\frac{dx_i}{dt} = (x_{i+1} - x_{i-2})x_{i-1} - x_i + 8, \quad (19)$$

where we have periodic boundary conditions (so $x_{-1} = x_{s-1}$, $x_0 = x_s$, $x_{s+1} = x_1$). The choice of forcing constant $F = 8$ induces chaotic behaviour, and is typical for data assimilation applications. In the experiments presented in Section 7.2 we use the numerical implementation of [10], where the model is integrated in time with a fourth-order Runge–Kutta scheme. For all experiments we consider $N = 15$ subwindows.

As we are interested in assessing the performance of preconditioners within the linearised inner loops, we consider a single outer loop of the weak constraint formulation. As the model (19) is non-linear, applying the weak constraint 4D-Var implementation requires the computation of the tangent linear model (or linearisation of the forward model), \mathbf{M}_i , and adjoint model, \mathbf{M}_i^{AD} , at each subwindow, $i = 1, \dots, 15$. We note that the adjoint linearisation is not the transpose of the tangent linear model, i.e. $(\mathbf{M}_i^{AD})^\top \neq \mathbf{M}_i$, and \mathbf{M} itself is not symmetric.

Additionally, for this problem the linearised model \mathbf{M}_i is different at each subwindow, i.e. $\mathbf{M}_i \neq \mathbf{M}_{i+1}$. For larger time-steps Δt the difference between subsequent model linearisations increases. We also note that as \mathbf{M}_i is not symmetric, its eigenvalues have non-zero imaginary part. An important assumption in the theory presented in Section 4 was that the spectral radius of \mathbf{M} is bounded above by 1. For Lorenz 96, the spectral radius of \mathbf{M}_i increases with i , and even when $\rho(\mathbf{M}_1) < 1$, we find that $\rho(\mathbf{M}_{15}) > 1$. In general the spectral radius of \mathbf{M}_i increases with i . For smaller model time-steps Δt the spectral radius approaches 1, and we obtain \mathbf{M}_i that are closer together for subsequent time-steps. We consider $\Delta t = 10^{-6}$ for all the experiments presented in Section 7.2, although similar results were obtained for other values of Δt and are not presented here.

The linearised model \mathbf{M}_i does not satisfy the assumptions that are required for the theory presented in Section 4. The Lorenz 96 example can therefore be considered as a study of how well the proposed preconditioners perform in a more general setting where these simplifying theoretical assumptions do not hold. As the saddle point matrix, \mathcal{A} , for this problem is not symmetric, a non-symmetric solver such as GMRES must be applied irrespective of the preconditioner. As the assumptions for the theoretical analysis of Section 4 do not apply for this problem, there is little reason to apply the block diagonal preconditioner. Hence, for this problem we only consider the inexact constraint preconditioner, \mathcal{P}_I .

6.3 Data assimilation parameters

We now describe the data assimilation problem that is studied for both problems in the experiments in Section 7. The size of the state space s is determined by the spatial discretisation $s = \frac{1}{\Delta x}$. For the heat equation we either observe 50% or 25% of observations at random, i.e. $p = \frac{s}{2}$ or $p = \frac{s}{4}$. For each choice of s we fix the observation operator $\mathbf{H} \in \mathbb{R}^{p \times N}$. The entries of \mathbf{H} are all 0 or 1, and each row has a single unit entry. The columns containing units are randomly selected for each choice of Δx and ordered. For the Lorenz 96 problem $p = \frac{s}{2}$, and observations of alternate state variables are smoothed equally over 5 adjacent state variables, with entries either being 0 or $\frac{1}{5}$.

We assume that the model error \mathbf{Q}_i is the same at each observation time, i.e. $\mathbf{Q}_i \equiv \mathbf{Q}$ for $i = 1, \dots, N$. Both \mathbf{B} and \mathbf{Q} are created using the same routine, based on a SOAR correlation matrix [41]. This routine constructs spatial local correlations whilst ensuring that the matrix has high sparsity. Both \mathbf{B} and \mathbf{Q} are circulant matrices fully defined by a single row. The number of non-zero entries in each row is fixed as 199 and 239 respectively, irrespective of the value of s . The non-zero entries are computed using a modified SOAR function following the procedure in [20]:

$$c_i = \sigma \left(1 + \frac{2|\sin(\frac{i\theta}{2})|}{L} \exp\left(-\frac{2|\sin(\frac{i\theta}{2})|}{L}\right) \right), \quad \theta = \frac{2\pi}{\text{maxval}},$$

where L is the correlation lengthscale (0.6 for \mathbf{B} , 0.5 for \mathbf{Q}), `maxval` determines the number of non-zero entries (100 for \mathbf{B} , 120 for \mathbf{Q}), and σ is the amplitude of the correlation function (0.4 for \mathbf{B} , 0.2 for \mathbf{Q}). To ensure positive definiteness of the function, if the smallest eigenvalue of the full matrix is negative a constant $\delta = |\lambda_{\min}(\mathbf{B})| + \eta$ is added to the diagonal, where η is a random number in $[0, 0.5]$.

The spatial structure for \mathbf{B} and \mathbf{Q} introduced above is similar to numerical frameworks that have been considered previously for weak-constraint data assimilation experiments [8, 10]. However, we note that for realistic data assimilation systems the true structure of \mathbf{Q} is not well known. Improved understanding of model error covariance matrices, and their estimation in preconditioners is of research interest, but will not be considered here. For our experiments we consider the use of the exact \mathbf{D} within the preconditioner, which is likely to lead to larger wallclock times for the block diagonal preconditioner (which requires the application of $\widehat{\mathbf{D}}^{-1}$). Similar techniques to those used to approximate $\widehat{\mathbf{R}}$ could be applied to \mathbf{D} , but this is left as future work.

Many experiments that account for correlated observation error covariance matrices use spatial correlations and circulant matrix structures (similar to those we are using for \mathbf{B}, \mathbf{Q}). However, in NWP error correlations often arise from satellite-based instruments which have interchannel uncertainty structures (see for instance [40, 33]), which appear as block structures within a matrix. Therefore for these experiments we construct a matrix with block structure, designed to replicate many of the properties of realistic interchannel error correlations.

To construct $\mathbf{R} \in \mathbb{R}^{p \times p}$ we define two vectors: `pvec` $\in \mathbb{R}^{\text{plen}}$ such that $p = \sum_{i=1}^{\text{plen}} \text{pvec}_i$ which gives the size of the blocks, and `pcorr` $\in \mathbb{R}^{\text{plen}(\text{plen}-1)/2}$ which gives the a multiplication factor for each off-diagonal block (note if `pcorr` _{i} = 0 the corresponding off-diagonal block is uncorrelated). Diagonal blocks are correlated and constructed as the Hadamard product of a sparse random matrix and a sparse SOAR matrix (using the same approach as for \mathbf{B} and \mathbf{Q} above). Off-diagonal blocks are sparse random matrices with entries in $(0, \text{pcorr}_i)$. The matrix \mathbf{R} is assembled by adding the diagonal blocks and upper half of the matrix and then symmetrising. This also increases the weight of the diagonal blocks. A similar approach to that used for \mathbf{B} and \mathbf{Q} is applied to guarantee that \mathbf{R} is positive definite, where if the minimum eigenvalue of \mathbf{R} is less than 1 it is increased to a small positive value. This value is fixed at 0.41, in order to control the conditioning of \mathbf{R} , and ensure that the condition numbers of \mathbf{D} and \mathbf{R} are comparable. This method of construction ensures we have adequate sparsity for high-dimensional experiments, that \mathbf{R} is positive definite with significant correlations, and that it is well-conditioned. In practice \mathbf{R} may be very ill-conditioned compared to \mathbf{D} , in which case we expect selecting a good choice of $\widehat{\mathbf{R}}$ would be even more vital to ensure fast convergence.

Finally, we wish to apply the reconditioning-inspired preconditioner for \mathbf{R} in an online way, with no parameter tuning by the user. One way to do this is to use the small eigenvalues of \mathbf{R} to select γ and T . For the ridge regression approach, we set $\gamma = \lambda_{\min}(\mathbf{R})$. For the minimum eigenvalue method we compute the smallest two eigenvalue–eigenvector pairs, and set the threshold equal to the second smallest, meaning only a single eigenvalue is changed. The small eigenvalues are computed using `eigs(R, 1, 'sr')` in MATLAB. For both approaches we use information from \mathbf{R} , but computing a small number of eigenvalues ensures this is computationally efficient. Finally, for all correlated choices of $\widehat{\mathbf{R}}$ we apply $\widehat{\mathbf{R}}^{-1}$ using the incomplete Cholesky factors computed with the MATLAB function `ichol` with the same sparsity structure as \mathbf{R} . For \mathbf{R}_{ME} this means the reconditioning method is applied as a low-rank update to the Cholesky factors via the Woodbury identity as this is more efficient in terms of storage.

Table 4: Minimum and maximum eigenvalues of preconditioned \mathbf{R} for different choices of $\widehat{\mathbf{R}}$ computed using the `eigs` function in MATLAB.

p	\mathbf{R}		$\mathbf{R}_{diag}^{-1}\mathbf{R}$		$\mathbf{R}_{block}^{-1}\mathbf{R}$		$\mathbf{R}_{RR}^{-1}\mathbf{R}$		$\mathbf{R}_{ME}^{-1}\mathbf{R}$
	λ_{\min}	λ_{\max}	λ_{\min}	λ_{\max}	λ_{\min}	λ_{\max}	λ_{\min}	λ_{\max}	λ_{\min}
125	0.4100	108.63	0.0131	2.7466	0.6779	1.3221	0.2908	1.0000	0.2602
250	0.4100	200.55	0.0077	3.3466	0.7886	1.2114	0.2908	1.0000	0.6021
500	0.4100	312.05	0.0061	4.4236	0.8889	1.1110	0.2908	1.0000	0.1129
1250	0.4100	540.99	0.0044	5.5440	0.9335	1.0665	0.2908	1.0000	0.1077
2500	0.4100	650.67	0.0055	6.0254	0.7556	1.2444	0.2908	1.0000	0.1302
5000	0.4100	706.94	0.0057	6.8106	0.6058	1.3941	0.2908	1.0000	0.1725

Table 4 shows the extreme eigenvalues of $\widehat{\mathbf{R}}^{-1}\mathbf{R}$ for each of the preconditioners discussed in Section 5. We recall that the maximum eigenvalue of $\mathbf{R}_{ME}^{-1}\mathbf{R}_{ME}$ is 1 by definition. We fix the smallest eigenvalue of \mathbf{R} , $\lambda_{\min}(\mathbf{R}) = 0.41$, to ensure that \mathbf{R} is well-conditioned. We see that the maximum eigenvalue of \mathbf{R} increases with p . Eigenvalues are more extreme for $\mathbf{R}_{diag}^{-1}\mathbf{R}$ than for any other preconditioned matrix. Including correlation information is beneficial in terms of the extreme eigenvalues. As the parameter choice for \mathbf{R}_{RR} only depends on the smallest eigenvalue of \mathbf{R} (which is fixed), the minimum and maximum eigenvalues of $\mathbf{R}_{RR}^{-1}\mathbf{R}$ do not change with increasing p . The block approach clusters both minimum and maximum eigenvalues of $\mathbf{R}_{block}^{-1}\mathbf{R}$ either side of 1, whereas the reconditioning approaches have a maximum preconditioned eigenvalue very close or equal to 1. For the approach used here, where T is set to the second smallest eigenvalue of \mathbf{R} , all eigenvalues bar the smallest of $\mathbf{R}_{ME}^{-1}\mathbf{R}$ are equal to 1.

7 Numerical experiments

In this section we present the results of the numerical experiments for the two problems described in Section 6. We use the MATLAB 2019b implementations of MINRES and GMRES; the convergence criteria is given by the relative residual in the two norm, and we use a tolerance of 10^{-6} for both problems of interest.

7.1 Numerical experiments for the heat equation

We now compare the performance of approximations $\widehat{\mathbf{L}}$ and $\widehat{\mathbf{R}}$ for the heat equation problem presented in Section 6.1. Table 5 shows terms from the bounds in Theorem 1 and the computed eigenvalues from the preconditioned system using the block diagonal preconditioner \mathcal{P}_D . As the condition number of \mathbf{D} appears in all terms of the bound, we consider the case where $\mathbf{B} = \mathbf{Q} = \mathbf{I}$. For problems where \mathbf{D} is ill-conditioned, we expect the bounds given by Theorem 1 to be weaker. In particular we expect the maximum and minimum eigenvalue bounds to become large in absolute value, and the upper bound on the largest negative eigenvalue to approach zero from below.

By design, the smallest positive eigenvalue of $\mathcal{P}_D^{-1}\mathcal{A}$ is bounded well away from zero, particularly for the choices of $\widehat{\mathbf{R}}$ that include correlation information. As Table 5 shows, the computed minimum positive eigenvalues behave in a similar way to the bound – the choice of $\widehat{\mathbf{R}}$ is most important, and for this example using \mathbf{R}_{block} bounds the eigenvalue furthest away from zero. The maximum negative eigenvalue is closer to zero than the minimum positive eigenvalue for all choices of $\widehat{\mathbf{L}}$ and $\widehat{\mathbf{R}}$. Including correlation information in $\widehat{\mathbf{R}}$ and model information in $\widehat{\mathbf{L}}$ moves the bound slightly away from zero. The computed maximum negative eigenvalues of $\mathcal{P}_D^{-1}\mathcal{A}$ are much more well bounded away from zero than indicated by the bounds. The biggest impact occurs when using \mathbf{L}_M instead of \mathbf{L}_0 , with minimal changes to the eigenvalues for different choices of \mathbf{R} . The computed eigenvalues of largest magnitude are smaller than the equivalent bounds, even for $\mathbf{D} = \mathbf{I}$. Using \mathbf{L}_M results in a smaller lower bound (larger upper bound) than using \mathbf{L}_0 for the smallest (largest) eigenvalue of $\mathcal{P}_D^{-1}\mathcal{A}$. This behaviour is also seen for the computed eigenvalues. Again, changing $\widehat{\mathbf{R}}$ makes less of a difference to the extreme eigenvalues than changing $\widehat{\mathbf{L}}$.

Figure 1 shows the performance of MINRES in terms of wallclock time and iteration count for the block diagonal preconditioner for each choice of $\widehat{\mathbf{L}}$ and $\widehat{\mathbf{R}}$. We find that using model information via \mathbf{L}_M leads to fewer iterations being required for convergence than using \mathbf{L}_0 . This also results in faster wallclock times. We also find that accounting for correlations in \mathbf{R} is crucial; using \mathbf{R}_{diag} leads to over double the number of iterations and much longer wallclock times than for any correlated choice of $\widehat{\mathbf{R}}$. Iteration count and wallclock times are very similar for the correlated choices of $\widehat{\mathbf{R}}$. This shows that the new approximations perform as well as the ‘ideal’ preconditioner

Table 5: *Top*: Bounds on negative and positive eigenvalues from Theorem 1 for $s = 250$, $N = 5$, $\mathbf{B} = \mathbf{Q} = \mathbf{I}$; *Bottom*: extreme negative and positive eigenvalues for this problem computed using the `eigs` function in MATLAB.

$\widehat{\mathbf{L}}$	$\widehat{\mathbf{R}}$	Lower bound	Bound on max -ve eval	Bound on min +ve eval	Upper bound
\mathbf{L}_0	\mathbf{R}_{diag}	-6.1618	-0.0003	0.0131	7.6927
\mathbf{L}_0	\mathbf{R}_{block}	-3.9540	-0.0292	0.6779	4.9914
\mathbf{L}_0	\mathbf{R}_{RR}	-3.5794	-0.0166	0.2908	4.2552
\mathbf{L}_0	\mathbf{R}_{ME}	-3.6203	-0.0118	0.2062	4.2554
\mathbf{L}_0	\mathbf{R}	-3.2554	-0.0551	1.0000	4.2554
\mathbf{L}_M	\mathbf{R}_{diag}	-6.9465	-0.0010	0.0131	8.4607
\mathbf{L}_M	\mathbf{R}_{block}	-4.4969	-0.0995	0.6779	5.5301
\mathbf{L}_M	\mathbf{R}_{RR}	-4.0525	-0.0574	0.2908	4.7251
\mathbf{L}_M	\mathbf{R}_{ME}	-4.0936	-0.0413	0.2062	4.7251
\mathbf{L}_M	\mathbf{R}	-3.72519	-0.1773	1.0000	4.7251
		$\lambda_{\min}(\mathcal{P}_D^{-1}\mathcal{A})$	$\max_{\lambda}(\lambda(\mathcal{P}_D^{-1}\mathcal{A}) < 0)$	$\min_{\lambda}(\lambda(\mathcal{P}_D^{-1}\mathcal{A}) > 0)$	$\lambda_{\max}(\mathcal{P}_D^{-1}\mathcal{A})$
\mathbf{L}_0	\mathbf{R}_{diag}	-1.5138	-0.0607	0.0417	2.7723
\mathbf{L}_0	\mathbf{R}_{block}	-1.5213	-0.0607	0.8139	2.5219
\mathbf{L}_0	\mathbf{R}_{RR}	-1.5191	-0.0607	0.5440	2.5171
\mathbf{L}_0	\mathbf{R}_{ME}	-1.5212	-0.0607	0.4308	2.5211
\mathbf{L}_0	\mathbf{R}	-1.5237	-0.0607	1.0000	2.5237
\mathbf{L}_M	\mathbf{R}_{diag}	-1.7786	-0.1923	0.0417	2.8857
\mathbf{L}_M	\mathbf{R}_{block}	-1.8063	-0.1917	0.8138	2.8068
\mathbf{L}_M	\mathbf{R}_{RR}	-1.7985	-0.1916	0.5436	2.7918
\mathbf{L}_M	\mathbf{R}_{ME}	-1.8062	-0.1916	0.4304	2.8061
\mathbf{L}_M	\mathbf{R}	-1.8087	-0.1916	1.0000	2.8087

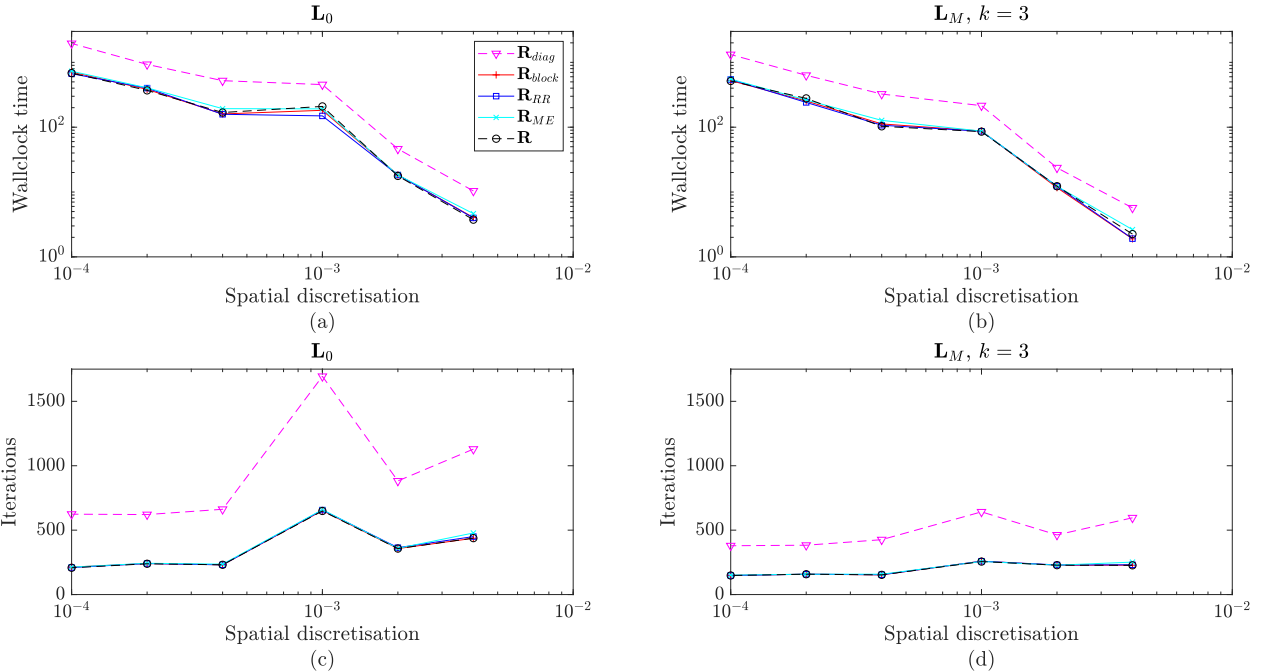


Figure 1: Number of iterations required for convergence and wallclock time (in seconds) of MINRES for (a,c) \mathbf{L}_0 and (b,d) \mathbf{L}_M for different choices of $\widehat{\mathbf{R}}$ for the block diagonal preconditioner for the heat equation. The dimension of the problem ranges from $\mathcal{A} \in \mathbb{R}^{3750 \times 3750}$ (right) to $\mathcal{A} \in \mathbb{R}^{150,000 \times 150,000}$ (left).

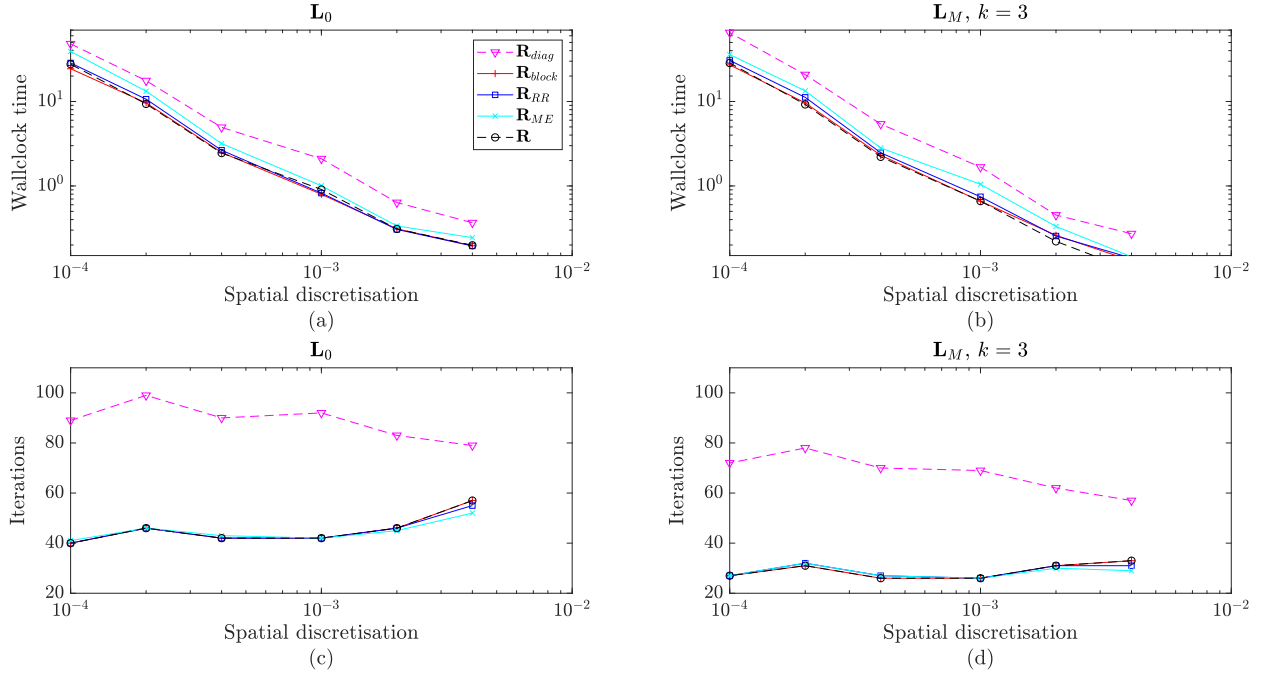


Figure 2: Number of iterations required for convergence and wallclock time (in seconds) of GMRES for (a,c) \mathbf{L}_0 and (b,d) \mathbf{L}_M for different choices of $\hat{\mathbf{R}}$ for the inexact constraint preconditioner for the heat equation. The dimension of the problem ranges from $\mathcal{A} \in \mathbb{R}^{3750 \times 3750}$ (right) to $\mathcal{A} \in \mathbb{R}^{150,000 \times 150,000}$ (left).

R. In general increasing the spatial and temporal discretisation yields a broadly similar number of iterations, particularly for \mathbf{L}_M , with increased wallclock times as expected.

Figure 2 shows the behaviour of GMRES in terms of iterations and wallclock time for the inexact constraint preconditioner and different choices of $\hat{\mathbf{L}}$ and $\hat{\mathbf{R}}$. We find that using the inexact constraint preconditioner results in far fewer iterations and much faster wallclock times than the block diagonal preconditioner. This agrees with prior experimental work for data assimilation problems where the inexact constraint approach performs well [18, 14, 15]. Similarly to the block diagonal case using \mathbf{L}_M compared to \mathbf{L}_0 leads to fewer iterations. However, as the reduction in iterations is smaller than for the block diagonal case, wallclock times are comparable for both \mathbf{L}_M and \mathbf{L}_0 for correlated choices of $\hat{\mathbf{R}}$, with longer wallclock times occurring for \mathbf{L}_M with \mathbf{R}_{diag} than \mathbf{L}_0 with \mathbf{R}_{diag} . Including correlation information in $\hat{\mathbf{R}}$ is beneficial in terms of both iterations and wallclock time, particularly for high-dimensional problems. There is some difference between the different choices of correlated $\hat{\mathbf{R}}$, however the behaviour of \mathbf{R}_{block} , \mathbf{R}_{RR} and \mathbf{R} is broadly similar. We note that these experiments are performed in serial, so we would expect faster wallclock times to be achievable for \mathbf{R}_{block} in a parallel implementation than the other choices of correlated $\hat{\mathbf{R}}$. Increasing the resolution of the problem results in improved convergence for the correlated choices of $\hat{\mathbf{R}}$, and an increase in wallclock times.

Fig 3 shows the behaviour of the inexact constraint preconditioner for high-dimensional problems. In particular for $\Delta x = 10^{-5}$ the dimension of the full saddle problem is $1,500,000 \times 1,500,000$ for $s = 4p$. We note that the size of the the time window is much smaller than for Figure 2 so the behaviour for $\Delta x = 10^{-4}$ is not directly comparable across the two experiments. We only consider the inexact constraint preconditioner and the three best choices of $\hat{\mathbf{R}}$. We find that even for a high-dimensional problem the number of iterations is small. Similarly to the lower dimensional case, using \mathbf{L}_M requires fewer iterations than using \mathbf{L}_0 . Wallclock time is also faster for \mathbf{L}_M than \mathbf{L}_0 . Convergence is very similar for the three choices of $\hat{\mathbf{R}}$, but there are differences in wallclock time, with \mathbf{R}_{RR} being the slowest. Figure 3 also considers two observation networks. We see that using a larger number of observations requires a larger number of iterations to reach convergence and longer wallclock time, which coincides with the findings of [8] for the unpreconditioned case. However, the qualitative behaviour across the different choices of $\hat{\mathbf{L}}$ and $\hat{\mathbf{R}}$ is the same for both observation networks.

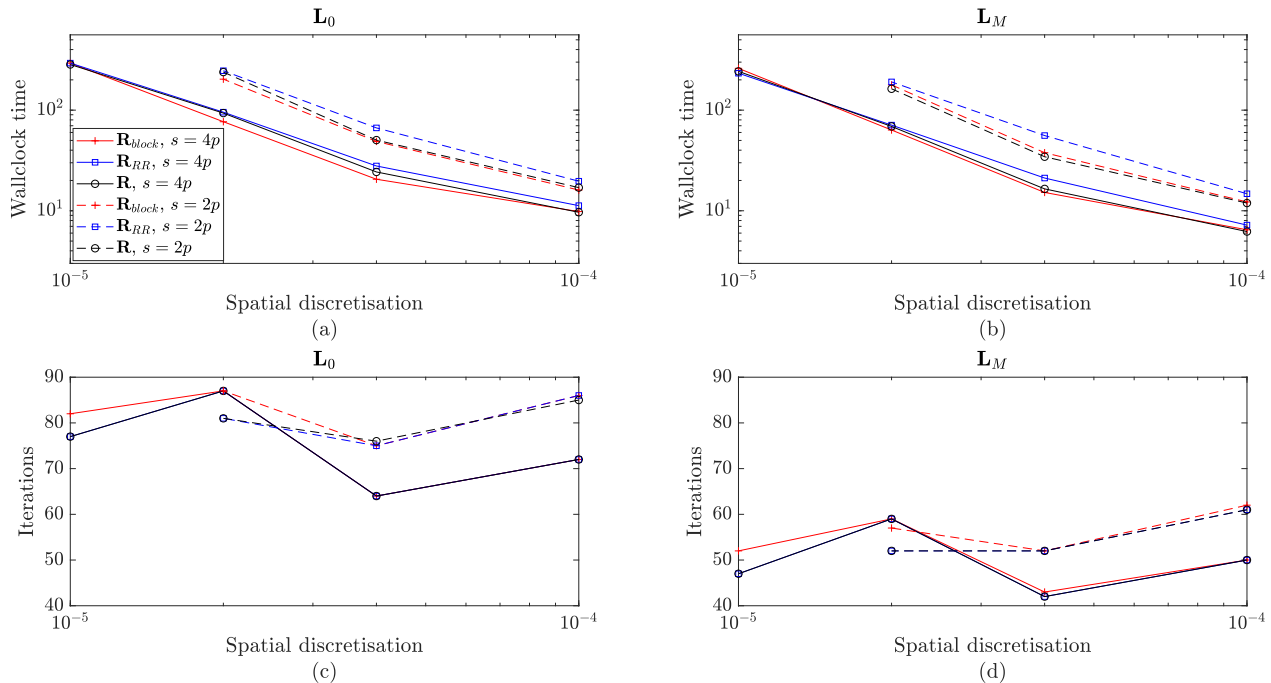


Figure 3: Number of iterations required for convergence and wallclock time (in seconds) for (a,c) \mathbf{L}_0 and (b,d) \mathbf{L}_M for different choices of $\hat{\mathbf{R}}$ for the inexact constraint preconditioner for large choices of s for the heat equation. Two observation ratios are shown: $p = \frac{s}{2}$ (dashed line) and $p = \frac{s}{4}$ (solid line). The dimension of the problem ranges from $\mathcal{A} \in \mathbb{R}^{150,000 \times 150,000}$ (right) to $\mathcal{A} \in \mathbb{R}^{750,000 \times 750,000}$ (left) for $p = \frac{s}{2}$ and $\mathcal{A} \in \mathbb{R}^{135,000 \times 135,000}$ (right) to $\mathcal{A} \in \mathbb{R}^{1,350,000 \times 1,350,000}$ (left) for $p = \frac{s}{4}$.

We therefore conclude that our new proposals for $\hat{\mathbf{L}}$ and $\hat{\mathbf{R}}$ are beneficial for both the block diagonal and inexact constraint preconditioners for this problem. In the block diagonal setting, using \mathbf{L}_M and correlated choices of $\hat{\mathbf{R}}$ lead to large decreases in iteration counts and decreases in wallclock time. For \mathcal{P}_I the use of \mathbf{L}_M decreases the number of iterations, but the changes in wallclock time are less significant than for the block diagonal case. Due to the fact that the inexact constraint preconditioner avoids the application of \mathbf{D}^{-1} the wallclock times are much faster for \mathcal{P}_I than for \mathcal{P}_D . However, we note that the wallclock times are strongly dependent on the efficiency of the numerical implementation. Therefore although the wallclock times can be used for comparison within the same experiment, iteration counts are more illustrative for comparison across different examples and choices of preconditioner.

Due to the large decrease in iteration counts and the fact that \mathcal{P}_I does not require the use of \mathbf{D}^{-1} , we recommend using the inexact constraint preconditioner even if the assumptions for the use of the block diagonal preconditioner are satisfied. We note that the qualitative behaviour for each of the preconditioners is similar across all experiments. Therefore, although the theoretical results of Sections 3 and 4 do not apply when using the inexact constraint preconditioner, the general conclusions from this theory are useful for designing improved terms within this preconditioner.

7.2 Numerical experiments for Lorenz 96

We now study the performance of the proposed choices of preconditioners for the Lorenz 96 problem presented in Section 6.2. Figure 4 shows how the number of iterations and wallclock time required for convergence change with the choice of $\hat{\mathbf{L}}$ and $\hat{\mathbf{R}}$ for \mathcal{P}_I as k increases. We see a clear benefit to including model information in terms of a reduction in iterations, even for small values of k . Increasing k leads to a reduction in the number of iterations required for convergence when using \mathbf{L}_M for all choices of $\hat{\mathbf{R}}$. Similarly to the heat equation setting, including correlation information in $\hat{\mathbf{R}}$ results in large improvements to convergence. In terms of iterations, there is very

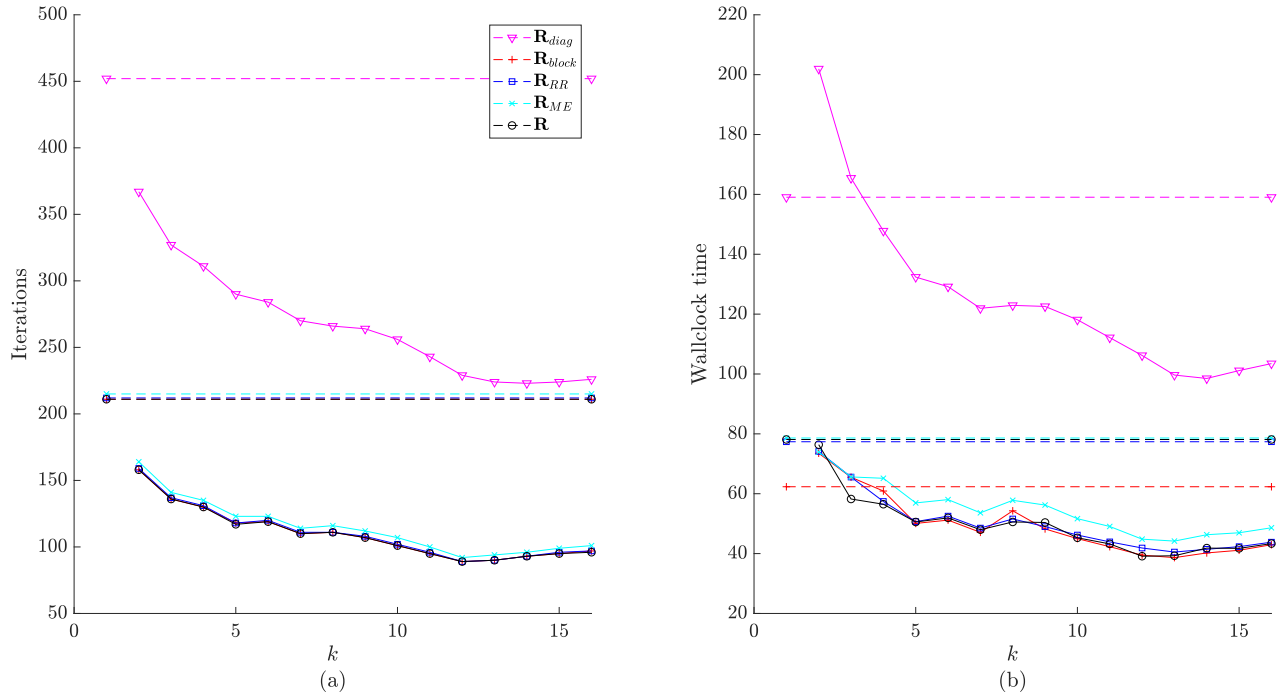


Figure 4: Number of iterations required for convergence for GMRES for (a) and wallclock time (in seconds; b) for the Lorenz 96 problem with increasing k for \mathbf{L}_0 (dashed lines) and \mathbf{L}_M (solid lines) and different choices of $\widehat{\mathbf{R}}$ for \mathcal{P}_I . The dimension of the problem is given by $\mathcal{A} \in \mathbb{R}^{100,000 \times 100,000}$.

little difference between the correlated choices of $\widehat{\mathbf{R}}$. In particular \mathbf{R}_{block} yields very similar performance to using the exact choice of \mathbf{R} . The reduction in iterations leads to improvements in wallclock time for $k \geq 4$ for all choices of $\widehat{\mathbf{R}}$ for \mathbf{L}_M compared to \mathbf{L}_0 . For \mathbf{L}_0 although the iteration count is very similar across all correlated choices of $\widehat{\mathbf{R}}$, the fastest wallclock time occurs for \mathbf{R}_{block} , as the cost of applying $\widehat{\mathbf{R}}^{-1}$ is the dominant cost for a single multiplication with the preconditioner. For \mathbf{L}_M the cost of a matrix–vector multiplication with the preconditioner is dominated by multiplications with \mathbf{L}_M^{-1} and $\mathbf{L}_M^{-\top}$. Therefore the wallclock times for the correlated choices of $\widehat{\mathbf{R}}$ are much more similar when including model information in the preconditioner. This implementation is designed to test the feasibility of new preconditioning approaches, and may not be sufficiently large to clearly highlight the full computational benefit of the block diagonal structure of \mathbf{R}_{block} , particularly in a serial implementation. We recall that \mathbf{R}_{block} has additional parallelisability that is not exploited in these serial experiments. For a larger problem with a parallel implementation we expect \mathbf{R}_{block} to be highly beneficial in terms of wallclock time as well as iteration count.

Table 6 shows the performance of the inexact constraint method for a higher-dimensional problem for \mathbf{R}_{block} , \mathbf{R}_{RR} , and \mathbf{R} . Similarly to the smaller dimensional problem considered in Figure 4, using \mathbf{L}_M leads to improved convergence in terms of iterations compared to \mathbf{L}_0 . Using \mathbf{R}_{block} requires slightly more iterations than \mathbf{R}_{RR} or \mathbf{R} , but we recall that \mathbf{R}_{block} has additional parallelisable structure. Increasing k leads to a slight reduction in the number of iterations, but increases the computational cost of each iteration. For this problem the best choice of k is therefore $k = 3$ which allows for maximum parallelisability and decreased iterations compared to \mathbf{L}_0 .

We therefore conclude that the qualitative behaviour seen for the linear heat problem also holds for the non-linear Lorenz 96 problem, even though none of the theoretical assumptions of Sections 3 and 4 apply. In particular using our new preconditioners \mathbf{L}_M and correlated choices of $\widehat{\mathbf{R}}$ result in fewer iterations and improved wallclock times than using \mathbf{L}_0 or \mathbf{R}_{diag} .

Table 6: Number of iterations required to reach convergence for the iterative constraint preconditioner applied to the Lorenz 96 problem, for GMRES for \mathbf{R}_{block} , \mathbf{R}_{RR} and \mathbf{R} for \mathbf{L}_0 and \mathbf{L}_M ($k = 3, 4, 5$). Here, $\mathcal{A} \in \mathbb{R}^{1,600,000 \times 1,600,000}$.

	\mathbf{R}_{block}	\mathbf{R}_{RR}	\mathbf{R}
\mathbf{L}_0	231	220	220
$\mathbf{L}_M, k = 3$	159	153	153
$\mathbf{L}_M, k = 4$	158	151	151
$\mathbf{L}_M, k = 5$	144	136	136

8 Conclusions

In this paper we have proposed new preconditioning approaches for the saddle point formulation of the weak-constraint 4D-Var data assimilation problem. In particular our new approach for approximating the model term, $\widehat{\mathbf{L}}$, incorporated model information for the first time. Additionally we proposed a variety of approaches that permit computationally efficient inclusion of correlation information within the observation error covariance term, $\widehat{\mathbf{R}}$.

In this paper:

- we developed new bounds for the eigenvalues of the preconditioned saddle point system in the case of a block diagonal preconditioner. The qualitative information can be used to assess the quality of preconditioners for each term, despite the bounds being weaker when \mathbf{D} is ill-conditioned.
- we investigated how the constituent terms within the bounds behave for existing and proposed choices of $\widehat{\mathbf{L}}$ and $\widehat{\mathbf{R}}$. We find that our new approaches have beneficial spectral properties including many clustered eigenvalues and extreme eigenvalues that are bounded by moderate numbers.
- we considered two numerical examples: the heat equation (which satisfies the assumptions of the theoretical results) and the Lorenz 96 problem (which does not satisfy the assumptions). For both cases we found clear benefit in terms of iterations and wallclock time for incorporating correlated information in $\widehat{\mathbf{R}}$, and using model information in \mathbf{L}_M for both the block diagonal preconditioner with MINRES and the inexact constraint preconditioner with GMRES.

Similarly to other previous work [15, 18, 13], using an inexact constraint preconditioner performs much better than the block diagonal preconditioner in terms of both iterations and wallclock time. Although the theory developed in this paper only applies to the block diagonal setting, improvements to individual terms were also found to aid the efficiency of the inexact constraint preconditioner. Iterations when using \mathbf{R}_{block} are very close to those of \mathbf{R} , with large reductions in wallclock time for cases when the application of $\widehat{\mathbf{R}}^{-1}$ is the dominant computational cost. For problems where \mathbf{R} is very ill-conditioned, we would expect the improvements in performance to be even greater than in the experiments presented here.

We find that including additional model information in \mathbf{L}_M leads to reduced iterations, but increases the computational expense of each iteration. We therefore suggest that $k = 3$ is a sensible trade-off which allows for additional parallelisation while retaining the benefits of using model information. We note that \mathbf{L}_M and \mathbf{R}_{block} have highly parallelisable structures, which have not been exploited in these serial experiments. Future work for this problem includes developing efficient approximations of \mathbf{D} , multi-core implementations of our new preconditioners, and experiments within a full-scale operational NWP system.

Acknowledgements

We thank Adam El-Said for his code for the Lorenz 96 weak constraint 4D-Var assimilation problem. We gratefully acknowledge funding from the Engineering and Physical Sciences Research Council (EPSRC) grant EP/S027785/1.

References

- [1] M. Benzi, G. H. Golub, and J. Liesen. Numerical solution of saddle point problems. *Acta Numerica*, 14:1–137, 2005.

- [2] L. Bergamaschi, J. Gondzio, M. Venturin, and G. Zilli. Inexact constraint preconditioners for linear systems arising in interior point methods. *Computational Optimization and Applications*, 36(2-3):137–147, 2007.
- [3] L. Bergamaschi, J. Gondzio, M. Venturin, and G. Zilli. Erratum to: Inexact constraint preconditioners for linear systems arising in interior point methods. *Computational Optimization and Applications*, 49(2):401–406, 2011.
- [4] D. S. Bernstein. *Matrix Mathematics: Theory, Facts, and Formulas*. Princeton University Press, Princeton, N.J.; Oxford, UK, 2nd edition, 2009.
- [5] M. Bonavita, Y. Trémolet, E. Holm, S. T. K. Lang, M. Chrust, M. Janisková, P. Lopez, P. Laloyaux, P. de Rosnay, M. Fisher, et al. *A strategy for data assimilation*. European Centre for Medium Range Weather Forecasts, Reading, UK, 2017.
- [6] A. Carrassi, M. Bocquet, L. Bertino, and G. Evensen. Data assimilation in the geosciences: An overview of methods, issues, and perspectives. *Wiley Interdisciplinary Reviews: Climate Change*, 9(5):e535, 2018.
- [7] E.S. Cooper, S.L. Dance, J. Garcia-Pintado, N.K. Nichols, and P.J. Smith. Observation impact, domain length and parameter estimation in data assimilation for flood forecasting. *Environmental Modelling & Software*, 104:199 – 214, 2018.
- [8] I. Daužickaitė, A. S. Lawless, J. A. Scott, and P. J. Van Leeuwen. Spectral estimates for saddle point matrices arising in weak constraint four-dimensional variational data assimilation. *Numerical Linear Algebra with Applications*, 27(5):e2313, 2020.
- [9] A. El Akkraoui, Y. Trémolet, and R. Todling. Preconditioning of variational data assimilation and the use of a bi-conjugate gradient method. *Quarterly Journal of the Royal Meteorological Society*, 139(672):731–741, 2013.
- [10] A. El-Said. *Conditioning of the weak-constraint variational data assimilation problem for numerical weather prediction*. PhD thesis, University of Reading, 2015.
- [11] H. Elman, D. Silvester, and A. Wathen. *Finite Elements and Fast Iterative Solvers*. Oxford University Press, Oxford, UK, 2nd edition, 2014.
- [12] M. Fisher, S. Gratton, S. Gürol, Y. Trémolet, and X. Vasseur. Low rank updates in preconditioning the saddle point systems arising from data assimilation problems. *Optimization Methods and Software*, 33(1):45–69, 2018.
- [13] M. Fisher and S. Gürol. Parallelization in the time dimension of four-dimensional variational data assimilation. *Quarterly Journal of the Royal Meteorological Society*, 143(703):1136–1147, 2017.
- [14] M. A. Freitag and D. L. H. Green. A low-rank approach to the solution of weak constraint variational data assimilation problems. *Journal of Computational Physics*, 357:263–281, 2018.
- [15] S. Gratton, S. Gürol, E. Simon, and P. L. Toint. Guaranteeing the convergence of the saddle formulation for weakly constrained 4D-Var data assimilation. *Quarterly Journal of the Royal Meteorological Society*, 144(717):2592–2602, 2018.
- [16] S. Gratton, A. S. Lawless, and N. K. Nichols. Approximate Gauss–Newton methods for nonlinear least squares problems. *SIAM Journal on Optimization*, 18(1):106–132, 2007.
- [17] Serge Gratton, Ph L Toint, and J Tshimanga Ilunga. Range-space variants and inexact matrix-vector products in krylov solvers for linear systems arising from inverse problems. *SIAM journal on matrix analysis and applications*, 32(3):969–986, 2011.
- [18] D. Green. *Model order reduction for large-scale data assimilation problems*. PhD thesis, University of Bath, 2019.
- [19] S. Gürol, A. T. Weaver, A. M. Moore, A. Piacentini, H. G. Arango, and S. Gratton. B-preconditioned minimization algorithms for variational data assimilation with the dual formulation. *Quarterly Journal of the Royal Meteorological Society*, 140(679):539–556, 2014.

- [20] S. A. Haben. *Conditioning and preconditioning of the minimisation problem in variational data assimilation*. PhD thesis, Department of Mathematics and Statistics, University of Reading, 2011.
- [21] M. R. Hestenes and E. Stiefel. Methods of conjugate gradients for solving linear systems. *Journal of Research of the National Bureau of Standards*, 49(6):409–436, 1952.
- [22] R. A. Horn and C. R. Johnson. *Topics in Matrix Analysis*. Cambridge University Press, 1991.
- [23] Yu. A. Kuznetsov. Efficient iterative solvers for elliptic finite element problems on nonmatching grids. *Russian Journal of Numerical Analysis and Mathematical Modelling*, 10(3):187–211, 1995.
- [24] E. N. Lorenz. Predictability: a problem partly solved. In *Seminar on Predictability, 4-8 September 1995*, volume 1, pages 1–18, Reading, 1995. ECMWF.
- [25] M. F. Murphy, G. H. Golub, and A. J. Wathen. A note on preconditioning for indefinite linear systems. *SIAM Journal on Scientific Computing*, 21(6):1969–1972, 2000.
- [26] C. C. Paige and M. A. Saunders. Solution of sparse indefinite systems of linear equations. *SIAM Journal on Numerical Analysis*, 12(4):617–629, 1975.
- [27] E. M. Pinnington, E. Casella, S. L. Dance, A. S. Lawless, J. I. L. Morison, N. K. Nichols, M. Wilkinson, and T. L. Quaife. Investigating the role of prior and observation error correlations in improving a model forecast of forest carbon balance using four-dimensional variational data assimilation. *Agricultural and Forest Meteorology*, 228-229:299–314, 2016.
- [28] E. M. Pinnington, E. Casella, S. L. Dance, A. S. Lawless, J. I. L. Morison, N. K. Nichols, M. Wilkinson, and T. L. Quaife. Understanding the effect of disturbance from selective felling on the carbon dynamics of a managed woodland by combining observations with model predictions. *Journal of Geophysical Research: Biogeosciences*, 122(4):886–902, 2017.
- [29] F. Rawlins, S. P. Ballard, K. J. Bovis, A. M. Clayton, D. Li, G. W. Inverarity, A. C. Lorenc, and T. J. Payne. The Met Office global four-dimensional variational data assimilation scheme. *Quarterly Journal of the Royal Meteorological Society*, 133:347–362, 2007.
- [30] T. Rees. *Preconditioning iterative methods for PDE constrained optimization*. PhD thesis, University of Oxford, 2010.
- [31] T. Rees and A. J. Wathen. Preconditioning iterative methods for the optimal control of the Stokes equation. *SIAM Journal on Scientific Computing*, 33(5):2903–2926, 2009.
- [32] Y. Saad and M. H. Schultz. GMRES: A generalized minimal residual algorithm for solving nonsymmetric linear systems. *SIAM Journal on Scientific and Statistical Computing*, 7(3):856–869, 1986.
- [33] L. M. Stewart, S. L. Dance, and N. K. Nichols. Correlated observation errors in data assimilation. *International Journal for Numerical Methods in Fluids*, 56:1521–1527, 2008.
- [34] J. M. Tabcart, S. L. Dance, S. A. Haben, A. S. Lawless, N. K. Nichols, and J. A. Waller. The conditioning of least-squares problems in variational data assimilation. *Numerical Linear Algebra with Applications*, 25(5):e2165, 2018.
- [35] J. M. Tabcart, S. L. Dance, A. S. Lawless, N. K. Nichols, and J. A. Waller. The conditioning of least squares problems in preconditioned variational data assimilation. *arXiv preprint arXiv:2010.08416*, 2020.
- [36] J. M. Tabcart, S. L. Dance, A. S. Lawless, N. K. Nichols, and J. A. Waller. Improving the condition number of estimated covariance matrices. *Tellus A: Dynamic Meteorology and Oceanography*, 72(1):1–19, 2020.
- [37] Y. Trémolet. Accounting for an imperfect model in 4D-Var. *Quarterly Journal of the Royal Meteorological Society*, 132(621):2483–2504, 2006.
- [38] Y. Trémolet. Model-error estimation in 4D-Var. *Quarterly Journal of the Royal Meteorological Society*, 133(626):1267–1280, 2007.

- [39] Joanne A Waller, Javier García-Pintado, David C Mason, Sarah L Dance, and Nancy K Nichols. Assessment of observation quality for data assimilation in flood models. *Hydrology and Earth System Sciences*, 22(7):3983–3992, 2018.
- [40] P. P. Weston, W. Bell, and J. R. Eyre. Accounting for correlated error in the assimilation of high-resolution sounder data. *Quarterly Journal of the Royal Meteorological Society*, 140:2420–2429, 2014.
- [41] A. M. Yaglom. *Correlation Theory of Stationary and Related Random Functions, Volume I: Basic Results*. Springer-Verlag, New York, 1987.
- [42] F. Zhang. *Matrix Theory: Basic Results and Techniques*. Springer, 2nd edition, 2011.